Electronic Supplementary Material (ESI) for Dalton Transactions.
This journal is © The Royal Society of Chemistry 2014

Supporting Information

Enhanced Association for C_{70} over C_{60} with a Metal Complex with Corannulene Derivate Ligands

Celedonio M. Álvarez,[,†] Luis A. García–Escudero,[†] Raúl García-Rodriguez,[†] Jose M. Martín-Alvarez,[†] Daniel Miguel,[†] Víctor M. Rayón[‡]*

[†]GIR MIOMeT, IU CINQUIMA/Química Inorgánica, Facultad de Ciencias, Universidad de Valladolid, E-47005, Valladolid, Spain.

[‡]Departamento de Química Física y Química Inorgánica, Facultad de Ciencias, Universidad de Valladolid, E-47005, Valladolid, Spain

* To whom correspondence should be addressed. E-mail: celedonio.alvarez@uva.es.

Table of contents.

I. General procedures and experimental data.

Spectroscopic Characterization.

Figure S1. ^{1}H NMR spectrum of Pt(dppe)(CC-Cora)$_2$ (**1**) at 400 MHz in $CDCl_3$.

Figure S2. ^{31}P{^{1}H} NMR spectrum of Pt(dppe)(CC-Cora)$_2$ (**1**) at 162 MHz in $CDCl_3$.

Figure S3. 2-D HSQC spectrum of Pt(dppe)(CC-Cora)$_2$ (**1**) in $CDCl_3$.

Figure S4. 2-D COSY spectrum of Pt(dppe)(CC-Cora)$_2$ (**1**) in $CDCl_3$.

Figure S5. ^{13}C{^{1}H} NMR spectrum of Pt(dppe)(CC-Cora)$_2$ (**1**) at 100 MHz in $CDCl_3$.

Figure S6. ^{1}H NMR spectrum of Pt(dppe)(CC-Pyrene)$_2$ (**2**) at 400 MHz in $CDCl_3$.

Figure S7. ^{31}P{^{1}H} NMR spectrum of Pt(dppe)(CC-Pyrene)$_2$ (**2**) at 162 MHz in $CDCl_3$.

Figure S8. 2-D COSY spectrum of Pt(dppe)(CC-Pyrene)$_2$ (**2**) in $CDCl_3$.

Figure S9. 2-D NOESY spectrum of Pt(dppe)(CC-Pyrene)$_2$ (**2**) in $CDCl_3$.

Figure S10. ^{13}C{^{1}H} NMR spectrum of Pt(dppe)(CC-Pyrene)$_2$ (**2**) at 100 MHz in $CDCl_3$.

Figure S11. ^{1}H NMR spectrum of Pt(dppe)(CC-hexahelicene)$_2$ (**3**) at 400 MHz in $CDCl_3$.

Figure S12. 2-D COSY spectrum of Pt(dppe)(CC-hexahelicene)$_2$ (**3**) in $CDCl_3$.

Figure S13. 2-D ROESY spectrum of Pt(dppe)(CC-hexahelicene)$_2$ (**3**) in $CDCl_3$.

Figure S14. ^{31}P{^{1}H} NMR spectrum of Pt(dppe)(CC-hexahelicene)$_2$ (**3**) at 162 MHz in THF-d$_8$.

Figure S15. ^{13}C{^{1}H} NMR spectrum of Pt(dppe)(CC-hexahelicene)$_2$ (**3**) at 100 MHz in $CDCl_3$.

Figure S16. ^{1}H NMR spectrum of Pt(dppe)(CC-CH$_2$-Cora)$_2$ (**4**) at 400 MHz in $CDCl_3$.

Figure S17. 2-D COSY spectrum of Pt(dppe)(CC-CH$_2$-Cora)$_2$ (**4**) in $CDCl_3$.

Figure S18. ^{31}P{^{1}H} NMR spectrum of Pt(dppe)(CC-CH$_2$-Cora)$_2$ (**4**) in $CDCl_3$ at 162 MHz.

Figure S19. 2-D HSQC spectrum of Pt(dppe)(CC-CH$_2$-Cora)$_2$ (**4**) in $CDCl_3$.

Figure S20. 2-D NOESY spectrum of Pt(dppe)(CC-CH$_2$-Cora)$_2$ (**4**) in $CDCl_3$.

Figure S21. ^{13}C{^{1}H} NMR spectrum of Pt(dppe)(CC-CH$_2$-Cora)$_2$ (**4**) at 100 MHz in $CDCl_3$.

II. Complexation studies.

Figure S22. Job plot showing the 1:1 stoichiometry of C_{60} *vs* **1** (on the left) and C_{70} *vs* **1** (on the right).

Figure S23. ^{1}H NMR titrations of [Pt(CC-Cora)$_2$(dppe)] (**1**) with C_{60} (400 MHz, 298 K, toluene-d$_8$).

Figure S24. Non linear curve regression for the results of the titration experiments of C_{60} with **1** for selected corannulene protons.

Figure S25. ^{13}C NMR (100 MHz) spectra of a mixture of C_{60} and **1** (1:1) in toluene-d$_8$ at several temperatures.

Figure S26. MALDI-TOF isotopic pattern for C60⊂**1**.

Figure S27. Partial ^{1}H NMR titrations of [Pt(CC-Cora)$_2$(dppe)] (**1**) with C_{70} (400 MHz, 298 K, toluene-d$_8$).

Figure S28. Non linear curve regression for the results of the titration experiments of C_{60} with **1** for selected corannulene protons.

Figure S29. MALDI-TOF isotopic pattern for C70⊂1.

III. Crystallographic Data for C60⊂1.

Crystallographic Experimental Section.

Table S1. Crystal data and structure refinement for C60⊂**1**.

Table S2. Bond lengths [Å] and angles [º] for C60⊂**1**.

IV. Computational details.

Figure S29. The three posible conformations of the **1**⊂C70 adduct as obtained at the BLYP-D3/TZP level of theory.

General notes and Procedures. Synthetic procedures were carried out under an inert atmosphere of nitrogen, in dry solvents (by passage through alumina columns in an IT Solvent Purification System and degassed with N_2), using standard Schlenk techniques, unless otherwise noted. All reagents and solvents were reagent grade and were used without further purification unless otherwise specified. Flash chromatographic purification was performed using silica gel Merck 60 (particle size 0.040–0.063 mm); the eluting solvent for each purification was determined by thin layer chromatography (TLC). Analytical thin-layer chromatography was performed using Merck TLC silica gel 60 F254. Trimethylsilylethynylcorannulene,[1] methylcorannulene,[2] 1-(trimethylsilylethynyl)pyrene,[3] and 9-bromoheptahelicene [4] were prepared according to the literature procedures and the spectral data in agreement with them. Solution NMR spectra were obtained on a Bruker AV-400 or a Varian MR 400 spectrometer, using $CDCl_3$ and toluene-d_8 as the solvents, internal lock, and internal reference (δ 7.26 (^{1}H) 77.16 (^{13}C) for $CDCl_3$) and (δ 2.08 (^{1}H) 20.43 (^{13}C) for toluene-d_8). Multiplicities are given as: s (singlet), br (broad), d (doublet), t (triplet), q (quartet), dd (doublet of doublets), m (multiplet); J coupling constants are given in Hz.

Synthesis of (bromomethyl)corannulene.

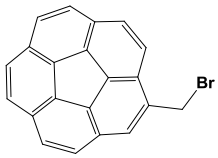

To methylcorannulene (100 mg, 0.38 mmol) in benzene (30 ml), N-bromosuccinimide (80 mg, 0.45 mmol) and benzoyl peroxide (5 mg) were added. The mixture was refluxed for 12 h. The organic layer was separated, washed with water, dried with magnesium sulphate, and evaporated. The product was purified by column chromatography on silica gel eluted with hexane/dichloromethane = 5/1 to yield (bromomethyl)corannulene as a white solid. (72 mg, 55%). ^{1}H NMR ($CDCl_3$, 400 MHz) δ 5.070 (s, 2**H**), 7.755 (d(AB system), *J* = 8.7 Hz, 1**H)**, 7.787 (d(AB system), *J* = 8.8 Hz, 1**H**), 7.804 (d(AB system), *J* = 8.7 Hz, 1**H**), 7.801 (d(AB system), *J* = 8.8 Hz, 1**H**), 7.817 (s(AB system), 2**H**), 7.830 (s, 1**H**), 7.894 (d(AB system), *J* = 9.0 Hz, 1**H**), 8.061 (d, *J* = 9.0 Hz, 1**H**). Anal. Calcd for $C_{21}H_{11}Br$: C, 73.49; H, 3.23. Found: 73.55; H 3.15.

Synthesis of [(trimethylsilylethynyl)methyl]corannulene.

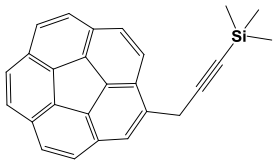

A schlenk tube was charged successively with Et_3N (30 mL), trimethylsilylacetylene (200 μL, 1.456 mmol), $Pd(PPh_3)_2Cl_2$ (20 mg, 0.028 mmol), CuI (6 mg, 0.028 mmol) and (bromomethyl)corannulene (100 mg, 0.29 mmol). The mixture was stirred vigorously at 85 ºC for 14 h., and then cooled, and the volatiles removed under reduced pressure. The product was purified by column chromatography on silica gel eluted with hexane/ethyl acetate = 20/1 to yield [(trimethylsilylethynyl)methyl]corannulene as a white solid. (89 mg, 85 %). ^{1}H NMR ($CDCl_3$, 400 MHz) δ 7.984 (d, *J* = 8.8 Hz, 1**H**), 7.855 (t, *J* = 1.0 Hz, 1**H**), 7.840 (d, *J* = 8.8 Hz, 1**H**), 7.811 (s(AB system), 2**H**), 7.801 (d(AB system), *J* = 8.8 Hz, 1**H**), 7.790 (s(AB system), 2**H**), 7.772 (d(AB system), *J* = 8.8 Hz, 1**H**), 4.176 (d, *J* = 1.0 Hz, 2**H**), 0.211 (s, 9**H**). Anal. Calcd for $C_{26}H_{20}Si$: C, 86.62; H, 5.59. Found: 86.55; H 5.60.

Synthesis of 9-(trimethylsilylethynyl)-[7]-helicene.

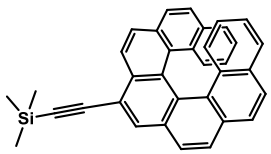

A schlenk tube was charged successively with Et_3N (15 mL), trimethylsilylacetylene (310 μL, 2.19 mmol), $Pd(PPh_3)_2Cl_2$ (31 mg, 0.044 mmol), CuI (10 mg, 0.044 mmol) and 9-bromoheptahelicene (200 mg, 0.437 mmol). The mixture was stirred vigorously at 85 ºC for 22 h., and then cooled, and the volatiles removed under reduced pressure. The product was purified by column chromatography on silica gel eluted with hexane/ethylacetate = 9/1 to yield 9-(trimethylsilylethynyl)-[7]-helicene as a white solid. (165 mg, 77 %). ^{1}H NMR ($CDCl_3$, 400 MHz) δ 8.565 (d, *J* = 8.4 Hz, 1**H**), 8.289 (s, 1**H**), 8.012 (d, *J* = 8.4 Hz, 1**H**), 7.940 (d(AB system), *J* = 8.1 Hz, 1**H**), 7.915 (d(AB system), *J* = 8.1 Hz, 1**H**), 7.751 (d, *J* = 8.6 Hz, 1**H**), 7.708 (d, *J* = 8.6 Hz, 1**H**), 7.508 (d, *J* = 8.4 Hz, 1**H**), 7.496 (d, *J* = 8.4 Hz, 1**H**), 7.300 (d, *J* = 8.6 Hz, 2**H**), 7.091 (d, *J* = 8.6 Hz, 1**H**), 7.058 (d, *J* = 8.6 Hz, 1**H**), 6.916 (t, *J* = 8.6 Hz, 1**H**), 6.908 (t, *J* = 8.6 Hz, 1**H**), 6.413 (t, *J* = 8.6 Hz, 2**H**), 0.430 (s, 9**H**). Anal. Calcd for $C_{35}H_{26}Si$: C, 88.56; H, 5.52. Found: 88.68; H 5.63.

Synthesis of Pt(dppe)(CC-Cora)$_2$ (1).

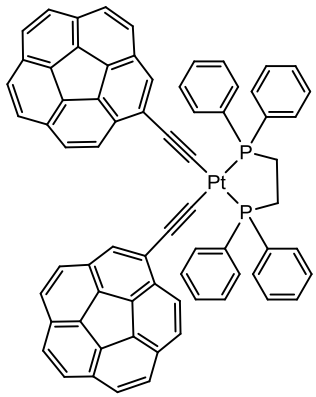

To a THF (15ml) solution of trimethylsilylethynylcorannulene (79 mg, 0.23 mmol) and $PtCl_2$dppe (73 mg 0.11 mmol) were added a solution of CuI (2mg) in acetonitrile (2 mL) and a methanol (5 mL) solution of KF (23 mg, 0.40 mmol) with stirring at room temperature for two days. The solution was concentrated by rotary evaporation to give the crude product, which was purified by silica gel column chromatography. Elution with dichlomethane – methanol (v/v = 99:1) gave a pale yellow product. (94 mg, 75%). ^{1}H NMR ($CDCl_3$, 400MHz) δ 8.07 – 8.00 (m, 8**H**, o-C_6H_5 dppe), 7.753 (d, *J* = 8.7 Hz, 2**H**, Cora), 7.751 (s, 2**H**, Cora), 7.745 (d(AB system), *J* = 8.8 Hz, 2**H**, Cora), 7.734 (s(AB system), 4**H**, Cora), 7.707 (d(AB system), *J* = 8.8 Hz, 2**H**, Cora), 7.683 (d(AB system), *J* = 8.8 Hz, 2**H**, Cora), 7.668 (d(AB system), *J* = 8.8 Hz, 2**H**, Cora), 7.640 (d, *J* = 8.7 Hz, 2**H**, Cora), 7.42 – 7.35 (m, 12**H**, m,p-C_6H_5 dppe), 2.56 – 2.36 (m, 4**H**, P(C*H*$_2$)$_2$P dppe); ^{1}H NMR (Tol-d8, 400MHz) δ 8.201 (d, *J* = 8.7 Hz, 2**H**, Cora), 8.00 - 7.92 (m, 8**H**, C_6H_5 dppe), 7.781 (s, 2**H**, Cora), 7.403 (d(AB system), *J* = 8.7 Hz, 2**H**, Cora), 7.402 (s(AB system), 4**H**, Cora), 7.355 (d(AB system), *J* = 8.7 Hz, 2**H**, Cora), 7.338 (d(AB system), *J* = 8.7 Hz, 2**H**, Cora), 7.294 (d, *J* = 8.7 Hz, 2**H**, Cora), 7.275 (d(AB system), *J* = 8.7 Hz, 2**H**, Cora), 7.05 – 6.95 (m, 12**H**, C_6H_5 dppe), 2.00 - 196 (m, 4**H**, P(C*H*$_2$)$_2$P dppe); ^{13}C{^{1}H} NMR ($CDCl_3$ 100 MHz) δ 136.08 ($C_{quaternary}$ Cora), 135.85 ($C_{quaternary}$ Cora), 135.50 ($C_{quaternary}$ Cora), 135.05 ($C_{quaternary}$ Cora), 134.05 ($C_{quaternary}$ Cora), 133.9 – 133.5 (m, C_α C_6H_5 dppe), 132.44 ($C_{quaternary}$ Cora), 131.5 – 131.3 (m, C_γ C_6H_5 dppe), 131.27 ($C_{quaternary}$ Cora), 130.77 ($C_{quaternary}$ Cora), 130.62 ($C_{quaternary}$ Cora), 130.30 ($C_{quaternary}$ Cora), 129.52 (d, $J_{P\text{-}C}$ = 55 Hz, C_{ipso} C_6H_5 dppe), 129.30 ($C_{tertiary}$ Cora), 129.1 – 128.8 (m, C_β C_6H_5 dppe), 128.27 ($C_{quaternary}$ Cora), 127.76 ($C_{tertiary}$ Cora), 126.90 ($C_{tertiary}$ Cora), 126.80 ($C_{tertiary}$ Cora), 126.76 ($C_{tertiary}$ Cora), 126.73 ($C_{tertiary}$ Cora), 126.69 ($C_{tertiary}$ Cora), 126.44 ($C_{tertiary}$ Cora), 126.34 ($C_{tertiary}$ Cora), 110.14 (dd, $J_{P\text{-}C(trans)}$ = 146 Hz, $J_{P\text{-}C(cis)}$ = 16 Hz, Pt-*C*≡C), 109.97 (d, $J_{P\text{-}C}$ = 35 Hz, Pt-C≡*C*), 29.07 – 28.45 (m, *C*H$_2$ dppe); ^{31}P{^{1}H} NMR ($CDCl_3$ 162 MHz) δ 42 (pseudo–t, $^1J_{P–Pt}$ = 2289 Hz). Anal. Calcd for $C_{70}H_{42}P_2Pt$: C, 73.74; H, 3.71. Found: 73.84; H 3.65.

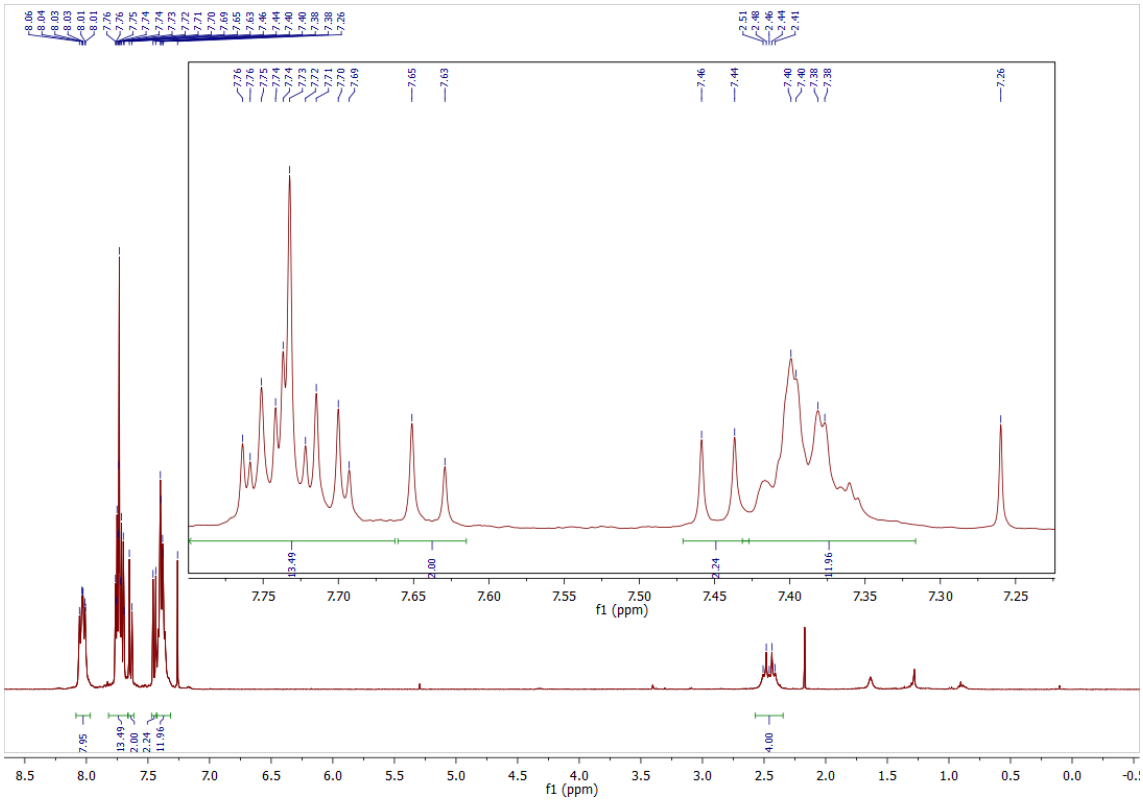

Figure S1. ^{1}H NMR spectrum of Pt(dppe)(CC-Cora)$_2$ (**1**) at 400 MHz in $CDCl_3$.

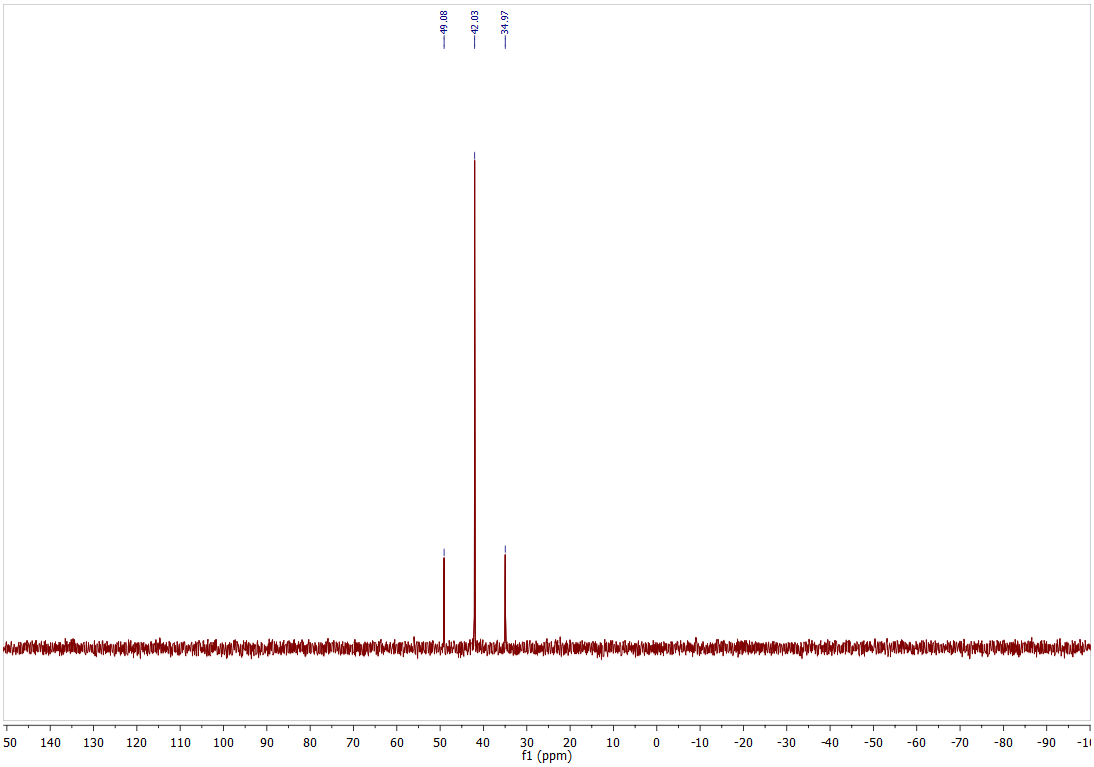

Figure S2. ^{31}P{^{1}H} NMR spectrum of Pt(dppe)(CC-Cora)$_2$ (**1**) at 162 MHz in $CDCl_3$.

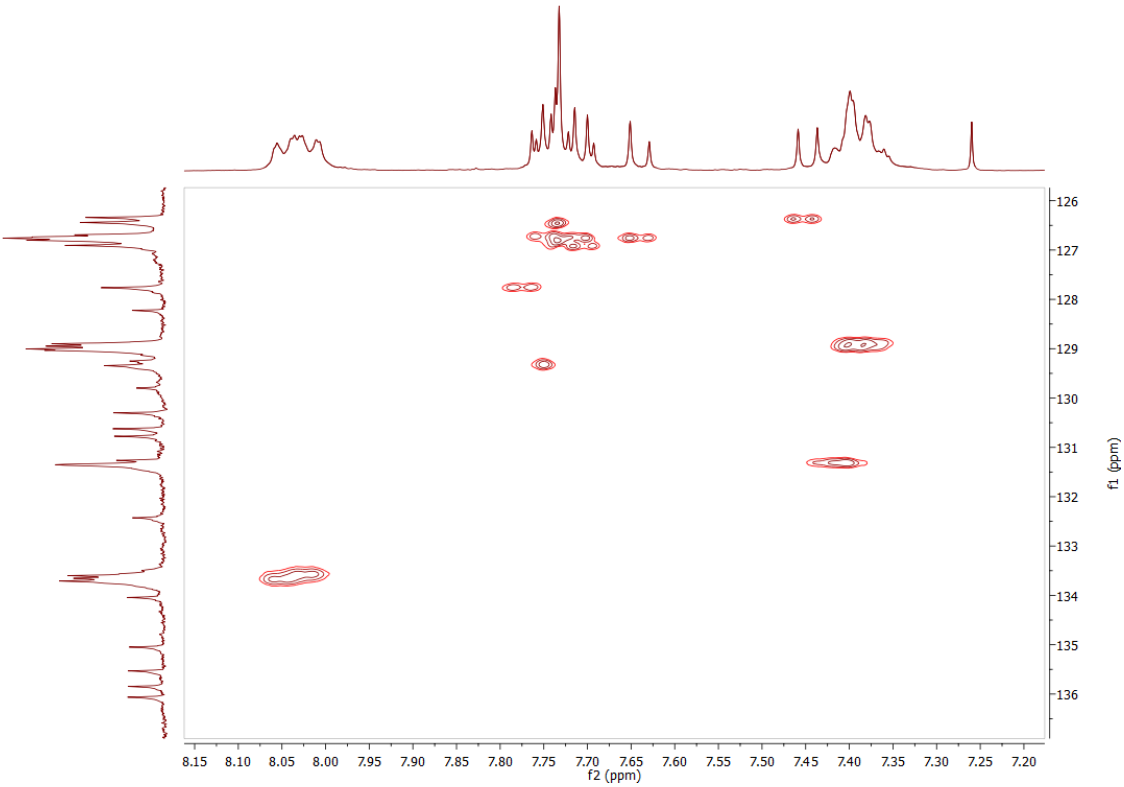

Figure S3. 2-D HSQC spectrum of Pt(dppe)(CC-Cora)$_2$ (**1**) in $CDCl_3$.

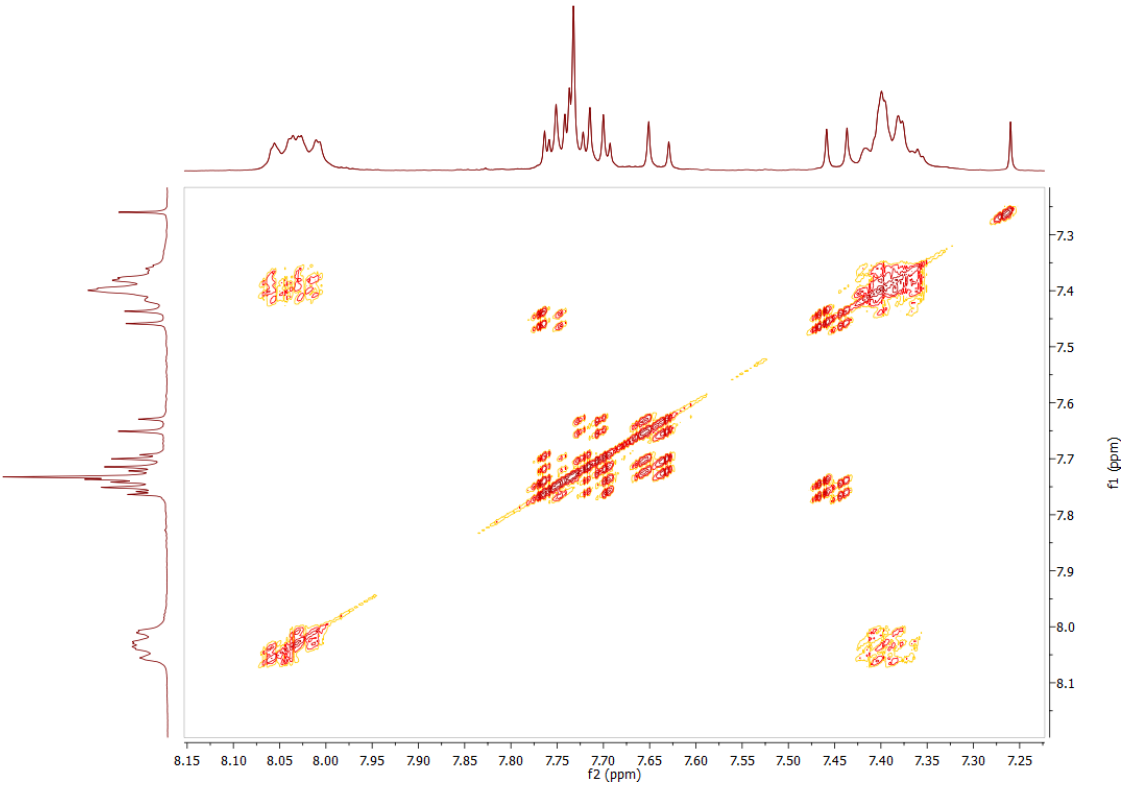

Figure S4. 2-D COSY spectrum of Pt(dppe)(CC-Cora)$_2$ (**1**) in $CDCl_3$.

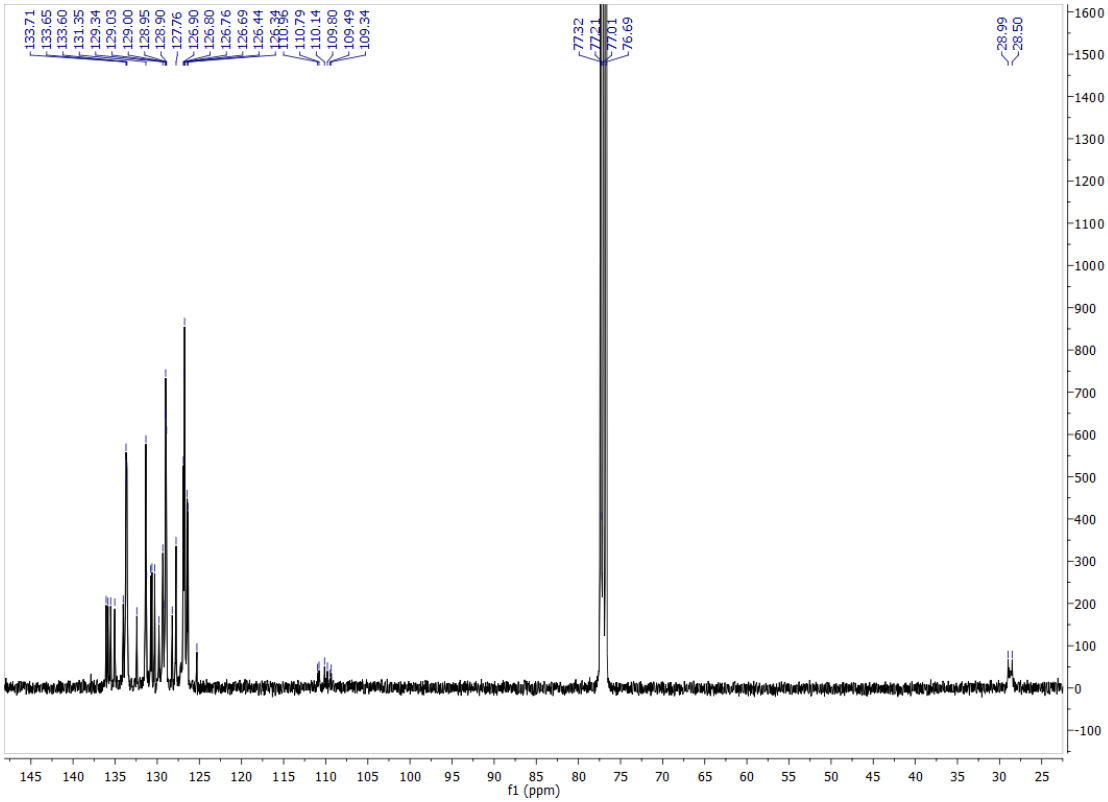

Figure S5. $^{13}C\{^{1}H\}$ NMR spectrum of Pt(dppe)(CC-Cora)$_2$ (**1**) at 100 MHz in $CDCl_3$.

Synthesis of Pt(dppe)(CC-Pyrene)$_2$ (2).

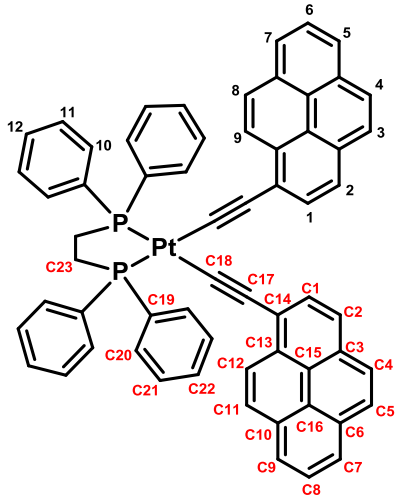

To a THF (15ml) solution of 1-(trimethylsilylethynyl)pyrene (103 mg, 0.345 mmol) and $PtCl_2$dppe (100 mg, 0.150 mmol) were added a solution of CuI (3 mg) in acetonitrile (2 mL) and a methanol (5 mL) solution of KF (32 mg, 0.54 mmol) with stirring at room temperature for five days. The solution was concentrated by rotary evaporation to give the crude product, which was purified by silica gel column chromatography. Elution with dichlomethane gave a pale yellow product. (122 mg, 80 %). ^{1}H NMR ($CDCl_3$, 400MHz) δ 8.58 (d, *J* = 9.1 Hz, 2**H**, H^9), 8.17 - 8.09 (m, 8**H**, H^{10}), 8.070 (d, *J* = 7.5 Hz, 2**H**, H^5), 8.027 (d, *J* = 7.5 Hz, 2**H**, H^7), 8.000 (d(AB system), *J* = 8.3 Hz, 2**H**, H^3 or H^4), 7.989 (d(AB system), *J* = 8.3 Hz, 2**H**, H^3 or H^4), 7.939 (d(AB system), *J* = 9 Hz, 2**H**, H^1 or H^2), 7.930 (d(AB system), *J* = 9 Hz, 2**H**, H^1 or H^2), 7.906 (pseudo-t (dd), *J* = 7.5 Hz, *J* = 7.5 Hz, 2**H**, H^6), 7.705 (d, *J* = 9.1 Hz, 2**H**, H^8), 7.53 – 7.43 (m, 12**H**, H^{11} and H^{12}), 2.64 – 2.47 (m, 4**H**, P(C*H*$_2$)$_2$P dppe); ^{13}C{^{1}H} NMR ($CDCl_3$ 100 MHz) δ 134.0 – 133.5 (m, C20), 131.84 (C13), 131.5 – 131.3 (m, C22 and C10), 130.14 (C4 or C5), 129.63 (d, *J* = 55 Hz, C19), 129.24 (C3), 129.1 – 128.8 (m, C21), 127.64 (C12), 127.39 (C1 or C2), 126.59 (C11), 126.48 (C1 or C2), 125.55 (C8), 124.63 (C6), 124.54 (C15), 124.41 (C9 and C16), 124.27 (C7), 124.23 (C4 or C5), 123.66 (C14), 111.49 (dd, *J* = 145 Hz, *J* = 15 Hz, C18), 110.90 (d, *J* = 35 Hz, C17), 29.0 – 28.4 (m, C23); ^{31}P{^{1}H} NMR (CDCl3 162 MHz) δ 42 (pseudo–t, $^1J_{P-Pt}$ = 2289 Hz). Anal. Calcd for $C_{62}H_{42}P_2Pt$: C, 71.33; H, 4.05. Found: 71.22; H 4.10.

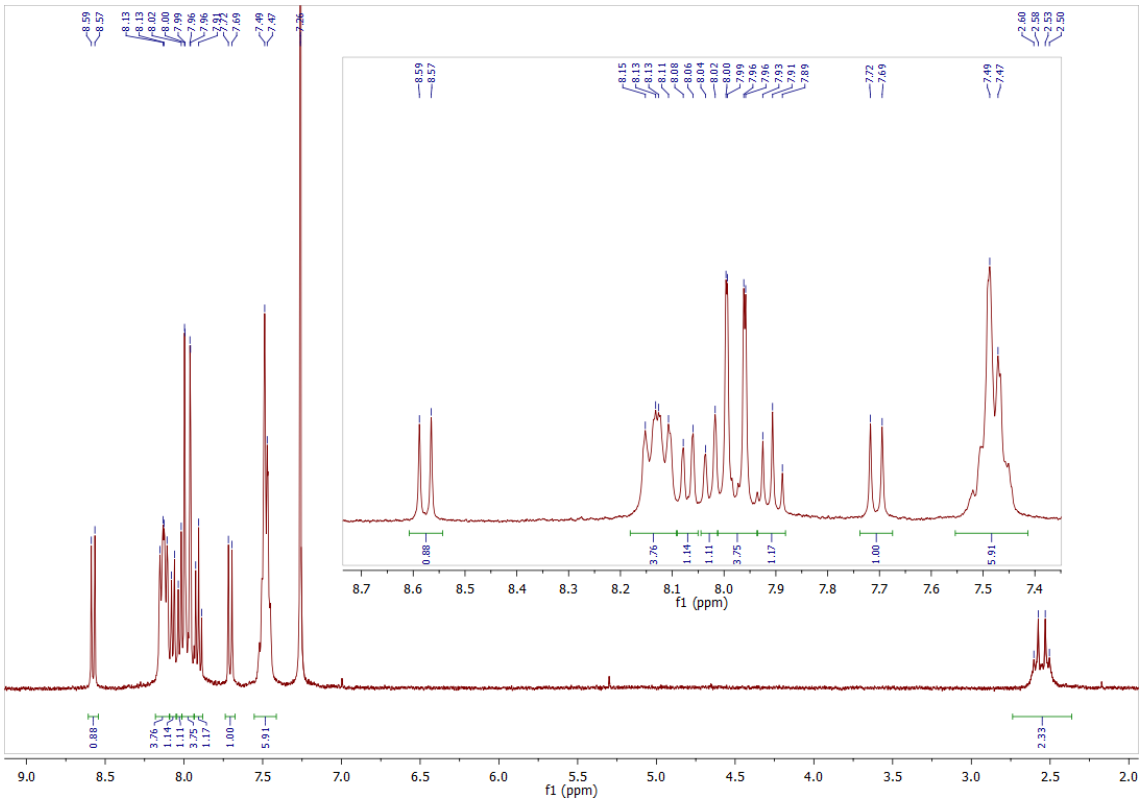

Figure S6. ^{1}H NMR spectrum of Pt(dppe)(CC-Pyrene)$_2$ (**2**) at 400 MHz in $CDCl_3$.

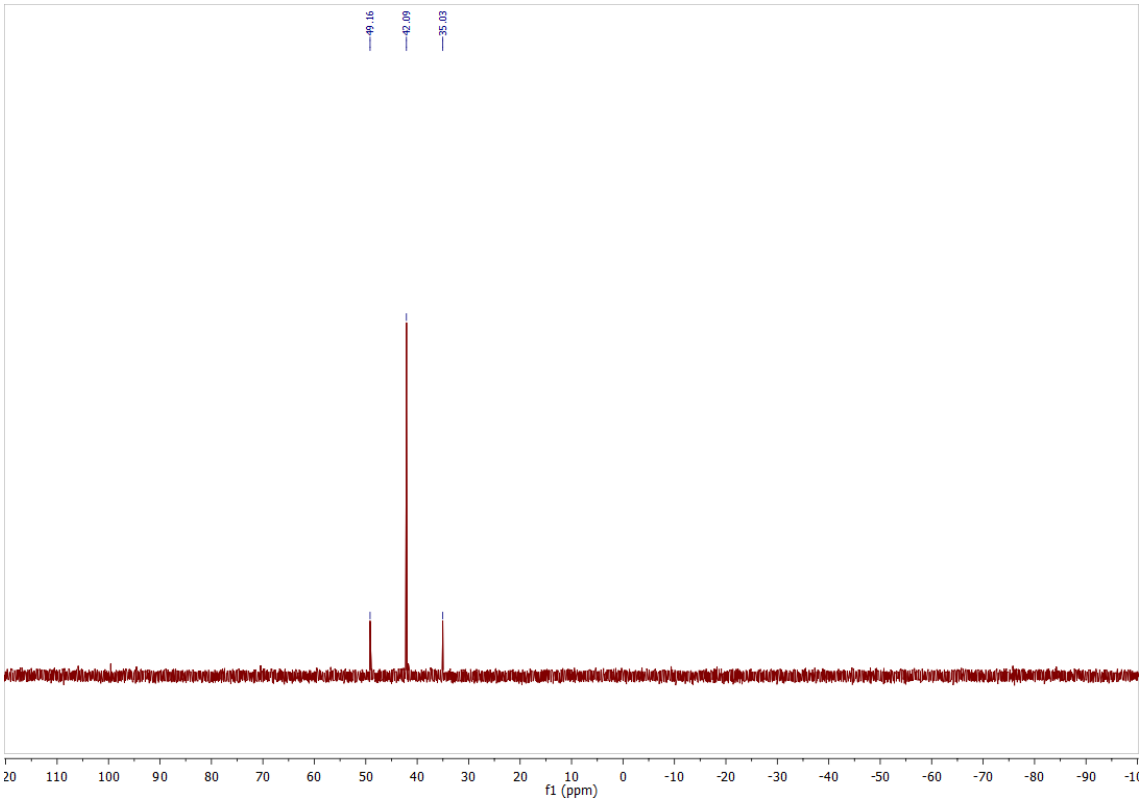

Figure S7. ^{31}P{^{1}H} NMR spectrum of Pt(dppe)(CC-Pyrene)$_2$ (**2**) at 162 MHz in $CDCl_3$.

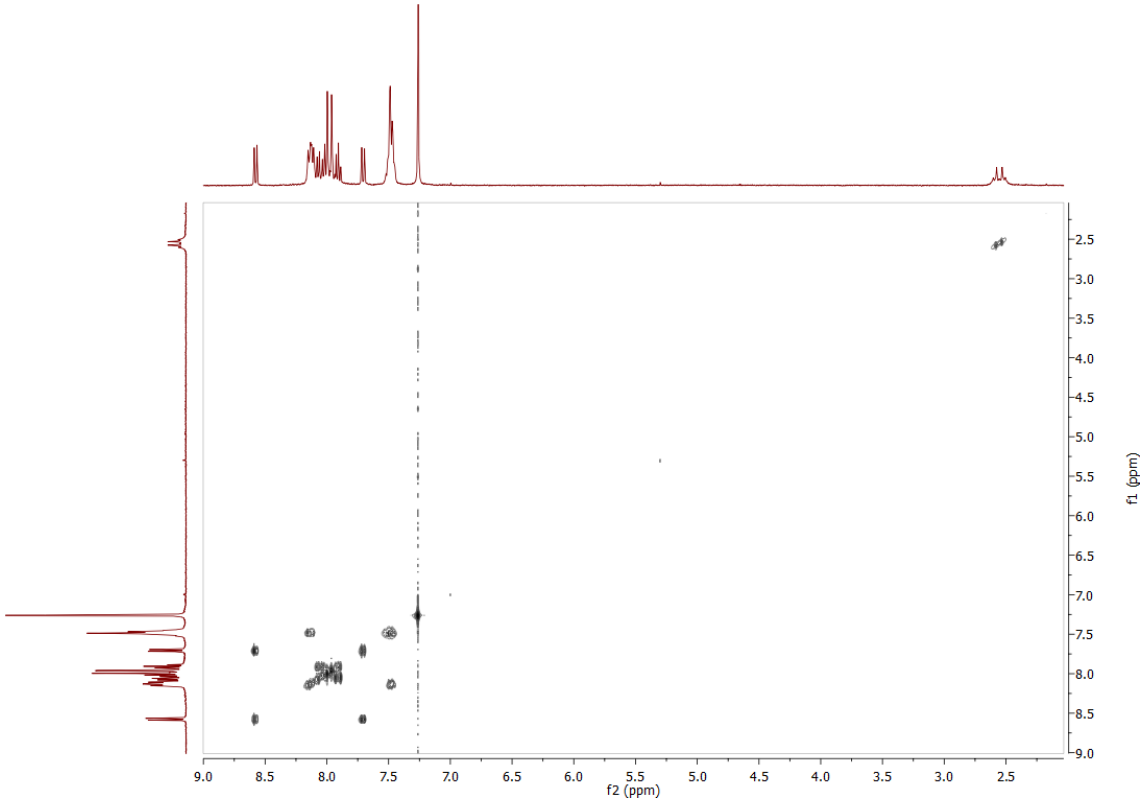

Figure S8. 2-D COSY spectrum of Pt(dppe)(CC-Pyrene)$_2$ (**2**) in $CDCl_3$.

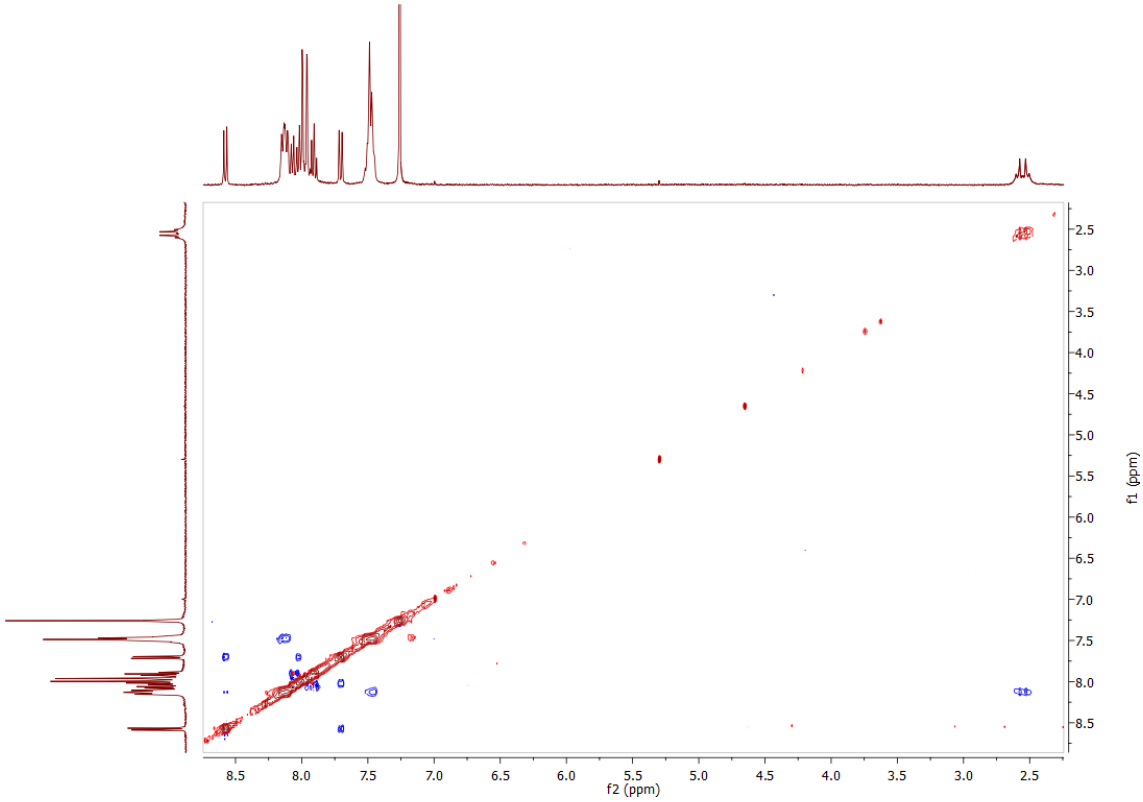

Figure S9. 2-D NOESY spectrum of Pt(dppe)(CC-Pyrene)$_2$ (**2**) in $CDCl_3$.

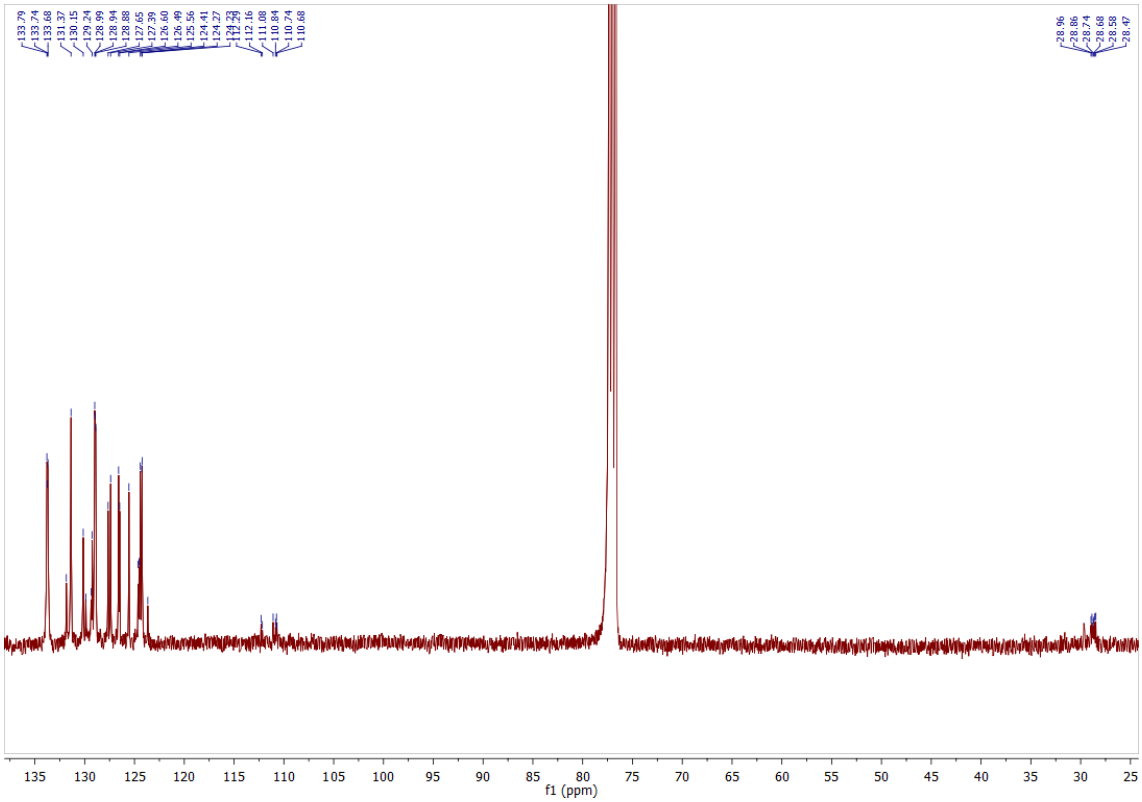

Figure S10. $^{13}C\{^{1}H\}$ NMR spectrum of Pt(dppe)(CC-Pyrene)$_2$ (**2**) at 100 MHz in $CDCl_3$.

Synthesis of Pt(dppe)(CC-hexahelicene)$_2$ (3).

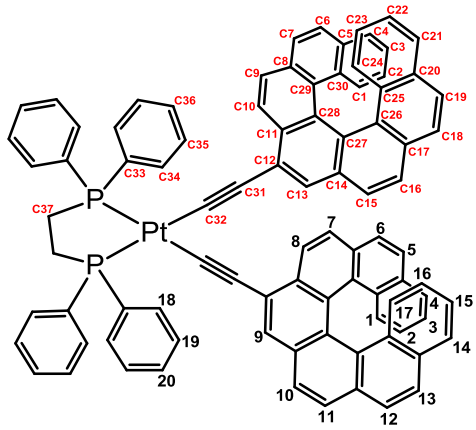

To a THF (15 ml) solution of 9-(trimethylsilylethynyl)-[7]-helicene (80 mg, 0.17 mmol) and $PtCl_2$dppe (25 mg, 0.072 mmol) were added a solution of CuI (2 mg) in acetonitrile (2 mL) and a methanol (5 mL) solution of KF (16 mg, 0.26 mmol) with stirring at room temperature for two days. The solution was concentrated by rotary evaporation to give the crude product, which was purified by silica gel column chromatography. Elution with dichlomethane gave a pale yellow product. (50 mg, 50 %). ^{1}H NMR ($CDCl_3$, 400MHz) δ 8.749 (d, J = 8.4 Hz, 2**H**, H^8), 8.18 - 8.10 (m, 8**H** H^{18}), 8.040 (s, 1**H**, H^9 (diastereomer A or B)), 8.034 (s, 1**H**, H^9 (diastereomer A or B)), 7.844 (d(AB system), J = 8.5 Hz, 2**H**, H^{10}), 7.830 (d(AB system), J = 8.5 Hz, 2**H**, H^{11}), 7.682 (d, J = 8.5 Hz, 2**H**, H^{12}), 7.592 (d, J = 8.6 Hz, 1**H**, H^5 or H^6 (diastereomer A or B)), 7.591 (d, J = 8.4 Hz, 1**H**, H^7 (diastereomer A or B)), 7.566 (d, J = 8.6 Hz, 1**H**, H^5 or H^6 (diastereomer A or B)), 7.565 (d, J = 8.4 Hz, 1**H**, H^7 (diastereomer A or B)), 7.54 – 7.48 (m, 12**H**, H^{19} and H^{20}), 7.435 (d, 8.5 Hz, 2**H**, H^{13}), 7.411 (d, J = 8.6 Hz, 1**H**, H^5 or H^6 (diastereomer A or B)), 7.402 (d, J = 8.6 Hz, 1**H**, H^5 or H^6 (diastereomer A or B)), 7.261 (d, J = 8.0 Hz, 4**H**, H^4 and H^{14}), 7.155 (d, J = 8.0 Hz, 2**H**, H^1 or H^{17}), 7.085 (d, J = 8.0 Hz, 1**H**, H^1 or H^{17} (diastereomer A or B)), 7.075 (d, J = 8.0 Hz, 1**H**, H^1 or H^{17} (diastereomer A or B)), 6.864 (pseudo-t (dd), J = 8.0 Hz, J = 8.0 Hz, 4**H**, H^3 and H^{15}), 6.376 (pseudo-t (dd), J = 8.0 Hz, 2**H**, H^2 or H^{16}), 6.343 (pseudo-t (dd), J = 8.0 Hz, 2**H**, H^2 or H^{16}), 2.62 – 2.41 (m, 4**H**, P(CH_2)$_2$P dppe); ^{13}C{^{1}H} NMR ($CDCl_3$ 100 MHz) δ 134.1 – 133.5 (m, C34), 133.04 (C11), 131.78 (C27 or C28), 131.65 (C20), 131.49 (C5), 131.4 – 131.3 (m, C36), 130.55 (C8), 130.49 (C17), 129.93 (C13), 129.72 (d, $J_{P\text{-}C}$ = 55 Hz, C33), 129.64 (C29 or C30), 129.42 (C25), 129.2 – 128.9 (m, C35), 128.40 (C26), 127.95 (C29 or C30), 127.15 (C15), 126.99 (C9), 126.97 (C6 or C7), 126.92 (C10), 126.79 (C6 or C7), 126.70 (C19), 126.60 (C16), 126.38 (C4 or C21), 126.35 (C4 or C21), 125.72 (C18 and C14), 125.19 (C12), 124.70 (C3 or C22), 124.65 (C1 or C24), 124.49 (C3 or C22), 124.37(C1 or C24), 123.89 (C27 or C28), 123.39 (C2 or C23), 123.32 (C2 or C23), 111.30 (dd, , $J_{P\text{-}C(trans)}$ = 145 Hz, $J_{P\text{-}C(cis)}$ = 15 Hz, C32), 109.88 (d, $J_{P\text{-}C}$ = 35 Hz, C31), 29.1 – 28.1 (m, C37); ^{31}P{^{1}H} NMR (CDCl3, 162 MHz) δ 42 (pseudo–t, $^1J_{P\text{–}Pt}$ = 2289 Hz); ^{31}P{^{1}H} NMR (THF-d8, 162 MHz) δ 42.33 (pseudo–t, $^1J_{P\text{–}Pt}$ = 2272 Hz, diastereomer A or B), 42.30 (pseudo–t, $^1J_{P\text{–}Pt}$ = 2272 Hz, diastereomer A or B). Anal. Calcd for $C_{62}H_{42}P_2Pt$: C, 77.41; H, 4.19. Found: 77.51; H 4.11.

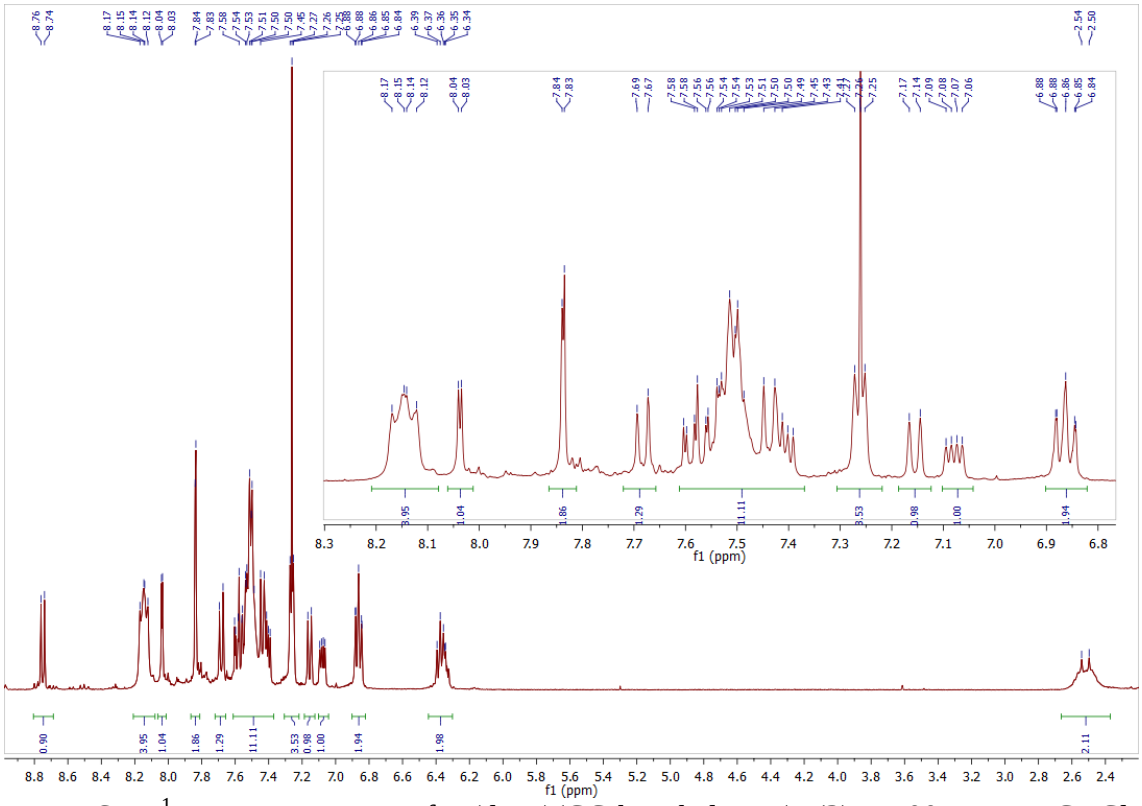

Figure S11. ^{1}H NMR spectrum of Pt(dppe)(CC-hexahelicene)$_2$ (**3**) at 400 MHz in $CDCl_3$.

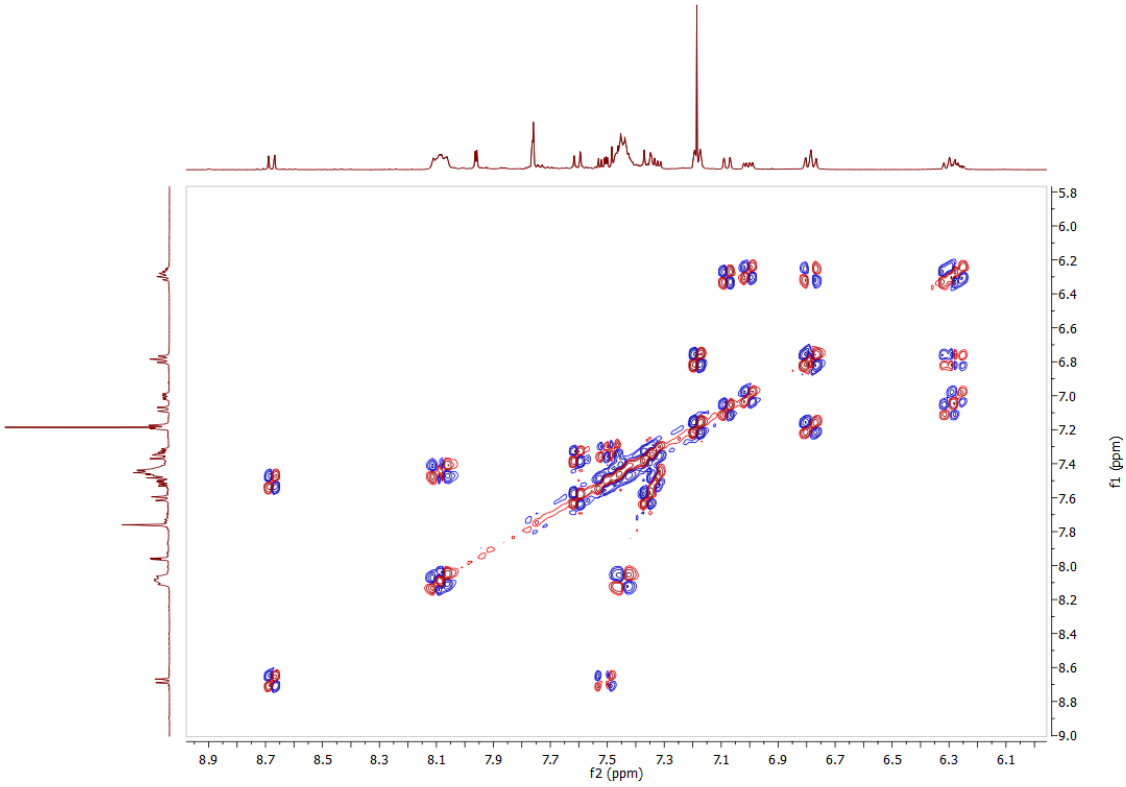

Figure S12. 2-D COSY spectrum of Pt(dppe)(CC-hexahelicene)$_2$ (**3**) in $CDCl_3$.

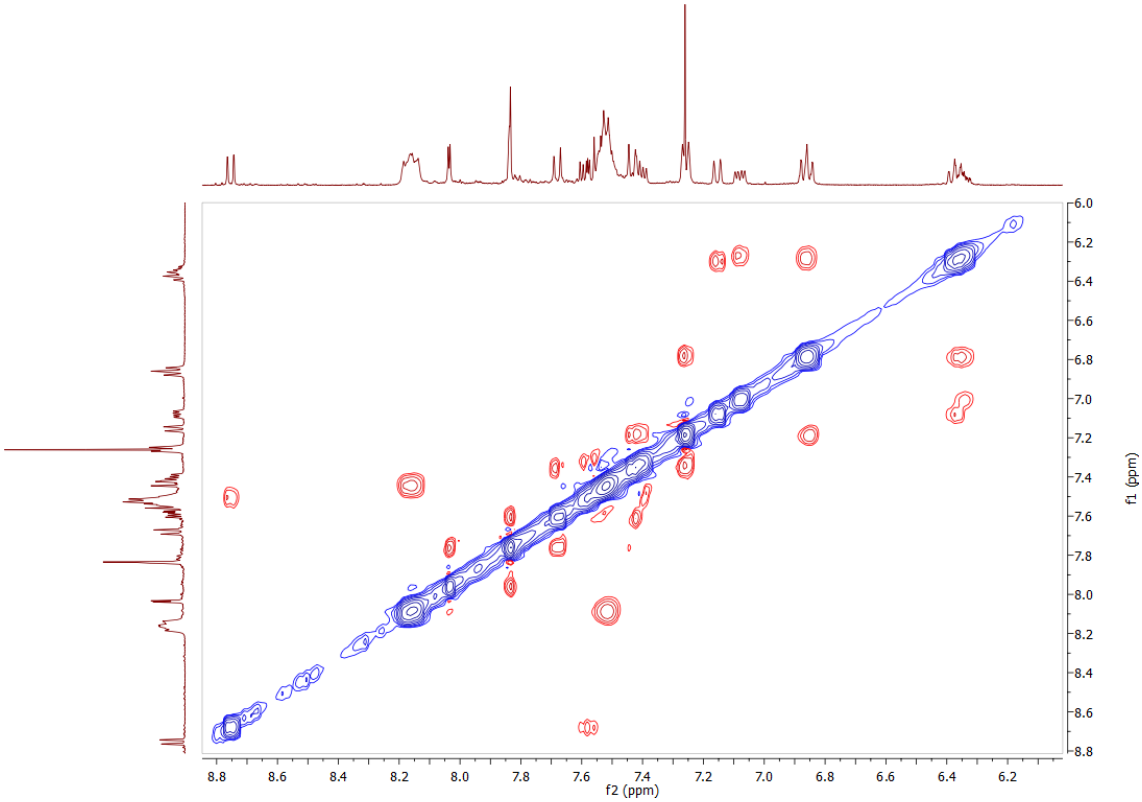

Figure S13. 2-D ROESY spectrum of Pt(dppe)(CC-hexahelicene)$_2$ (**3**) in $CDCl_3$.

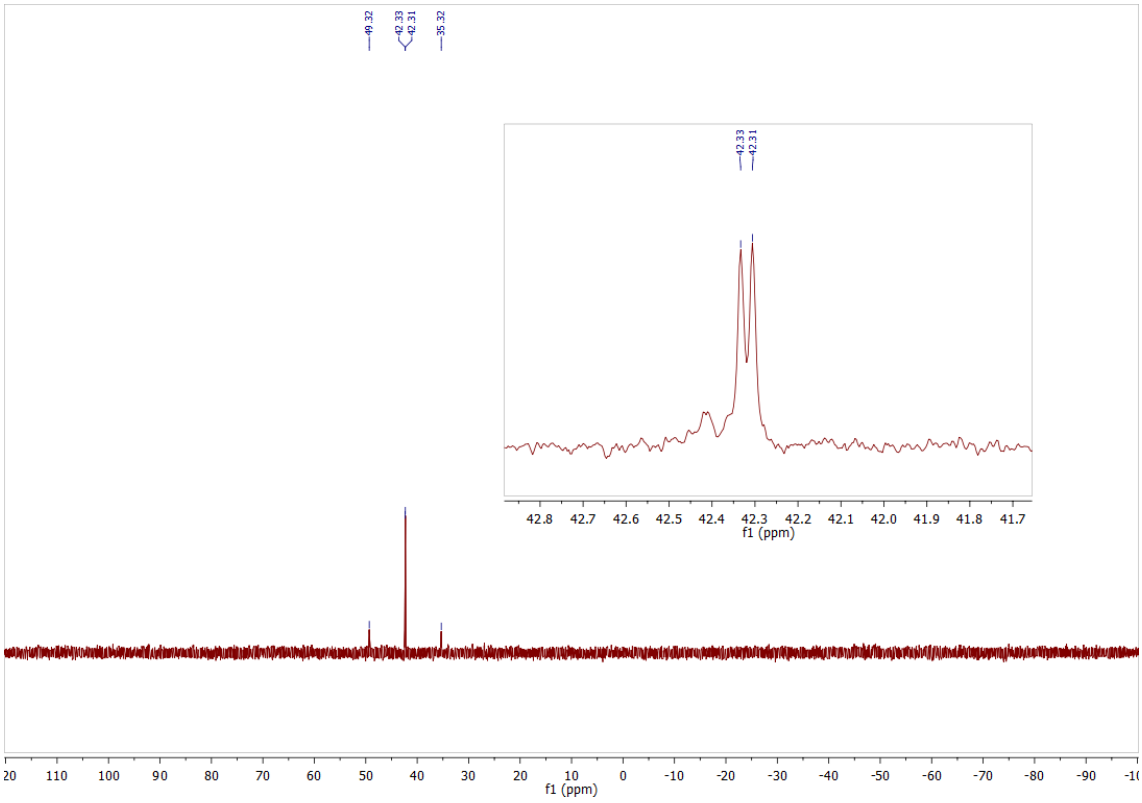

Figure S14. $^{31}P\{^1H\}$ NMR spectrum of Pt(dppe)(CC-hexahelicene)$_2$ (**3**) at 162 MHz in THF-d_8.

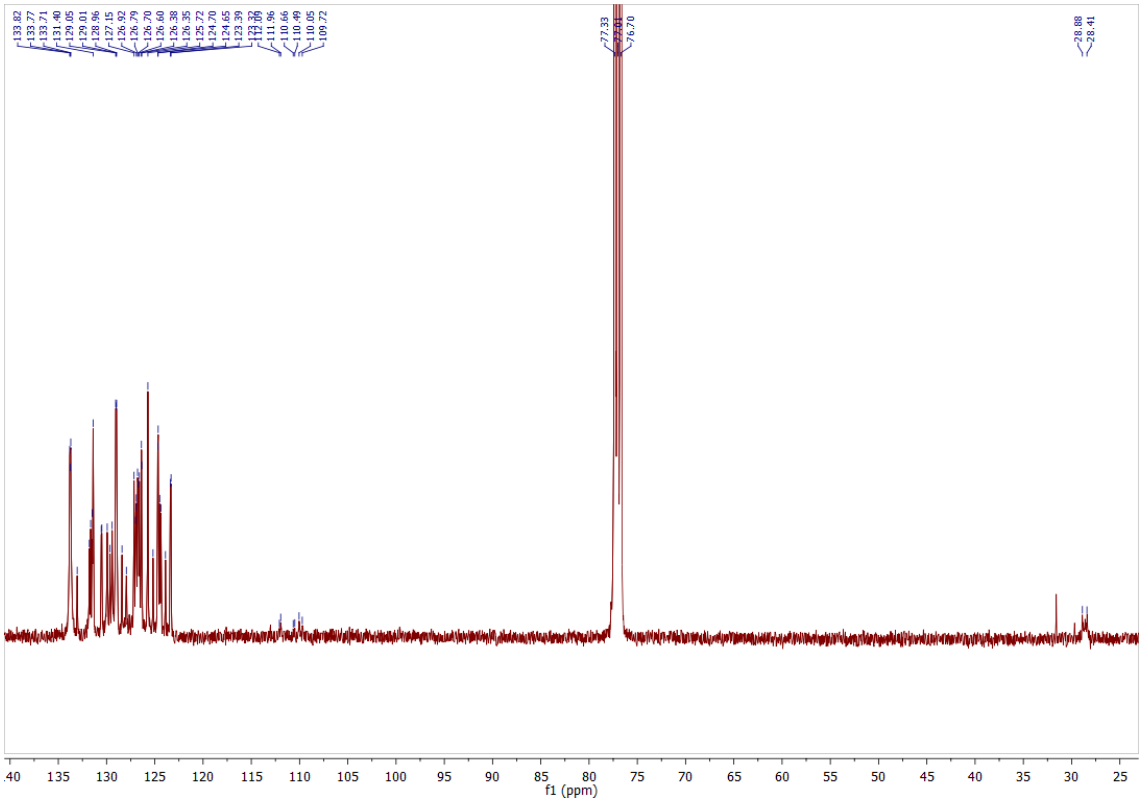

Figure S15. $^{13}C\{^{1}H\}$ NMR spectrum of Pt(dppe)(CC-hexahelicene)$_2$ (**3**) at 100 MHz in $CDCl_3$.

Synthesis of Pt(dppe)(CC-CH$_2$-Cora)$_2$ (4).

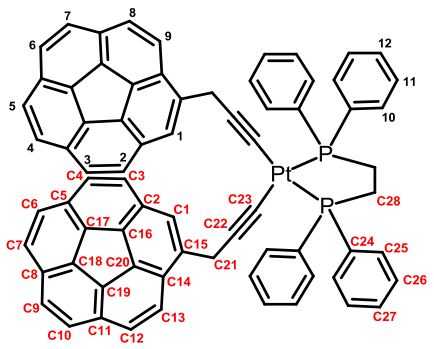

To a THF (10 ml) solution of [(trimethylsilylethynyl)methyl]corannulene (40 mg, 0.11 mmol) and PtCl$_2$dppe (32 mg, 0.048 mmol) were added a solution of CuI (1 mg) in acetonitrile (1 mL) and a methanol (2 mL) solution of KF (11 mg, 0.18 mmol) with stirring at room temperature for two days. The solution was concentrated by rotary evaporation to give the crude product, which was purified by silica gel column chromatography. Elution with dichlomethane gave a pale yellow product. (39 mg, 70 %). ^{1}H NMR (CDCl$_3$, 400MHz) δ 7.82 (d, *J* = 8.8 Hz, 2**H**; H^9), 7.76 (s(AB system), 4**H**; H^{4,5}), 7,74-7.66 (m, 8**H**; H^{10}), 7.73 (d, *J* = 8.7 Hz, 2**H**; H^6), 7.70 (t, *J* = 1.0 Hz, 2**H**; H^1), 7.64 (d, *J* = 8.8 Hz, 2**H**; H^3), 7.63 (d, *J* = 8.7 Hz, 2**H**; H^7), 7.39 (d, *J* = 8,8 Hz, 2**H**; H^2) 7.28 (d, *J* = 8.8 Hz, 2**H**; H^8), 6.90 (m, 4**H**; H^{12}), 6.81(m, 8**H**; H^{11}), 4.31 (m, 4**H**, C*H*$_2$-CC-), 2.50 (m, 4**H**, P(C*H*$_2$)$_2$P); ^{13}C{^{1}H} NMR (CDCl$_3$ 100 MHz) δ 138.59 (C15), 135.90 (C18), 135.69 (C17), 135.50 (C20), 135.28 (C19), 134.65 (C16), 133.7 – 133.0 (m, C25), 131.46 (C2), 130.7 – 130.6 (m, C27), 130.56 (C8), 130.39 (C14), 130.20 (C5 and C11), 128.93 (d, $J_{P\text{-}C}$ = 55 Hz, C24), 128.2 – 128.0 (m, C26), 127.23 (C3), 127.01 (C6 or C7), 126.85 (C10), 126.77 (C9), 126.59 (C4), 126.40 (C6 or C7), 126.33 (C12), 125.51 (C1), 1258.48 (C13), 108.24 (d, $J_{P\text{-}C}$ = 35 Hz, C22), 94.22 (dd, $J_{P\text{-}C(trans)}$ = 145 Hz, $J_{P\text{-}C(cis)}$ = 15 Hz, C23), 29.3 – 28.2 (m, C28), 25.93 (C21); ^{31}P{^{1}H} NMR (CDCl3 162 MHz) δ 41.2 (pseudo–t, $^1J_{P\text{–}Pt}$ = 2300 Hz). Anal. Calcd for C$_{72}$H$_{46}$P$_2$Pt: C, 74.03; H, 3.97. Found: 74.15; H 4.01.

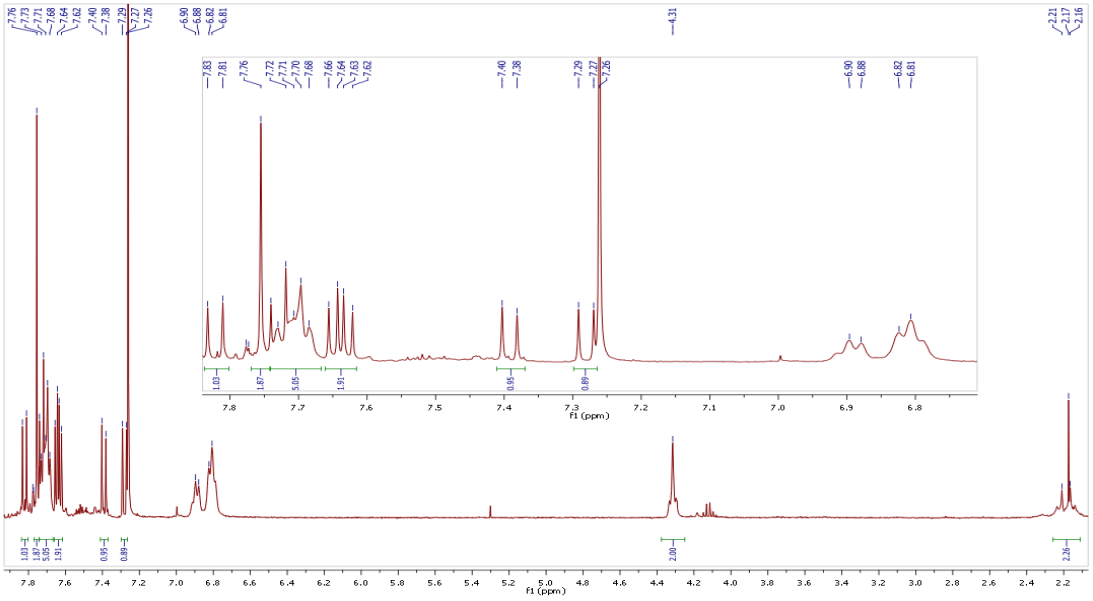

Figure S16. ^{1}H NMR spectrum of Pt(dppe)(CC-CH_2-Cora)$_2$ (**4**) at 400 MHz in $CDCl_3$.

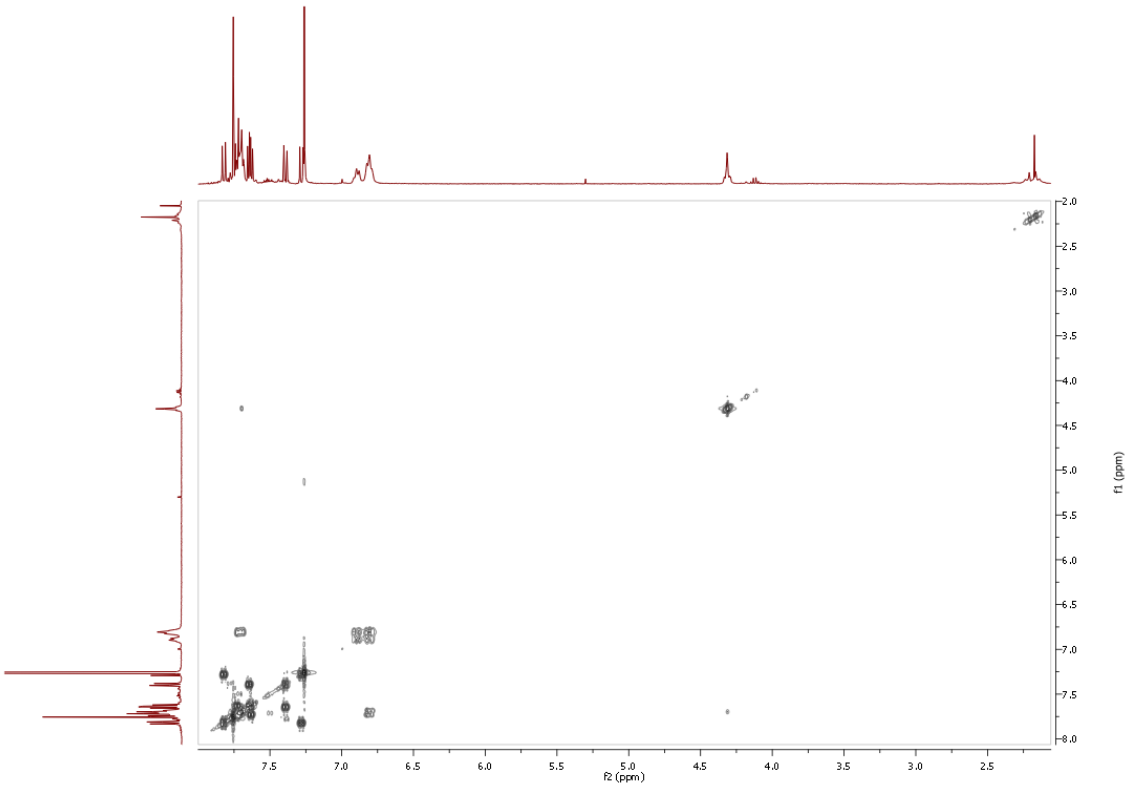

Figure S17. 2-D COSY spectrum of Pt(dppe)(CC-CH_2-Cora)$_2$ (**4**) in $CDCl_3$.

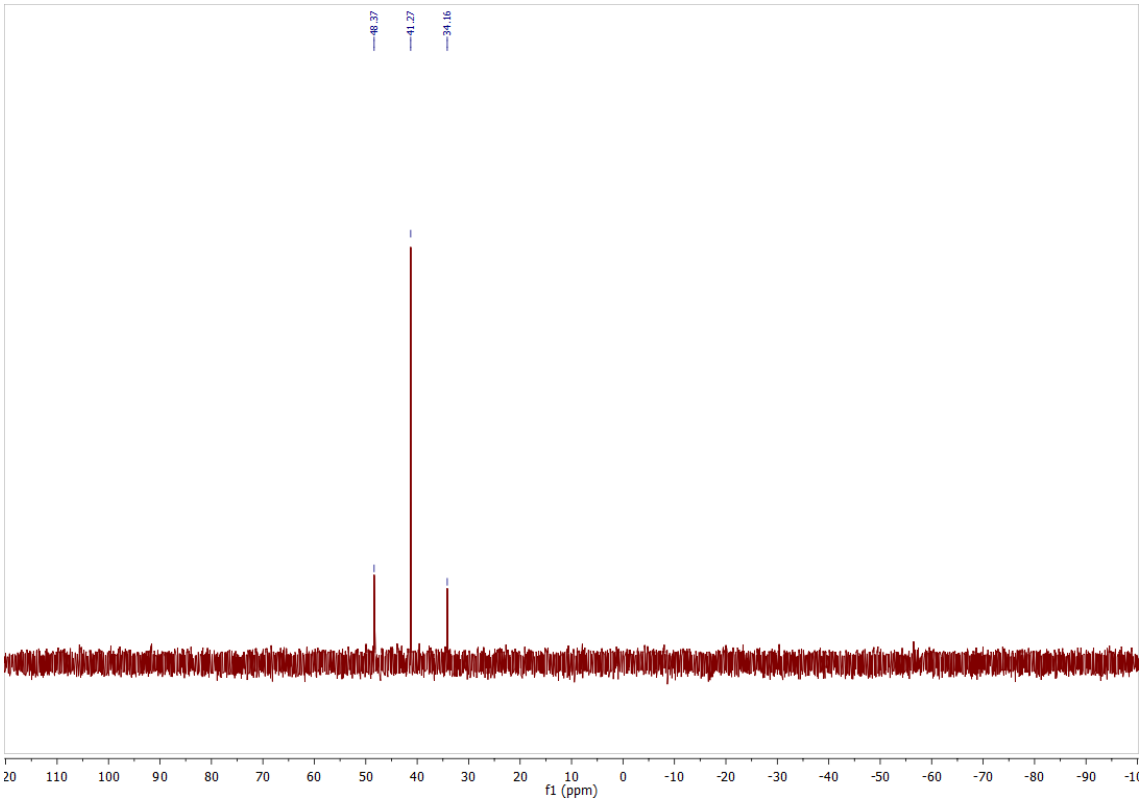

Figure S18. $^{31}P\{^{1}H\}$ NMR spectrum of Pt(dppe)(CC-CH_2-Cora)$_2$ (**4**) in $CDCl_3$ at 162 MHz.

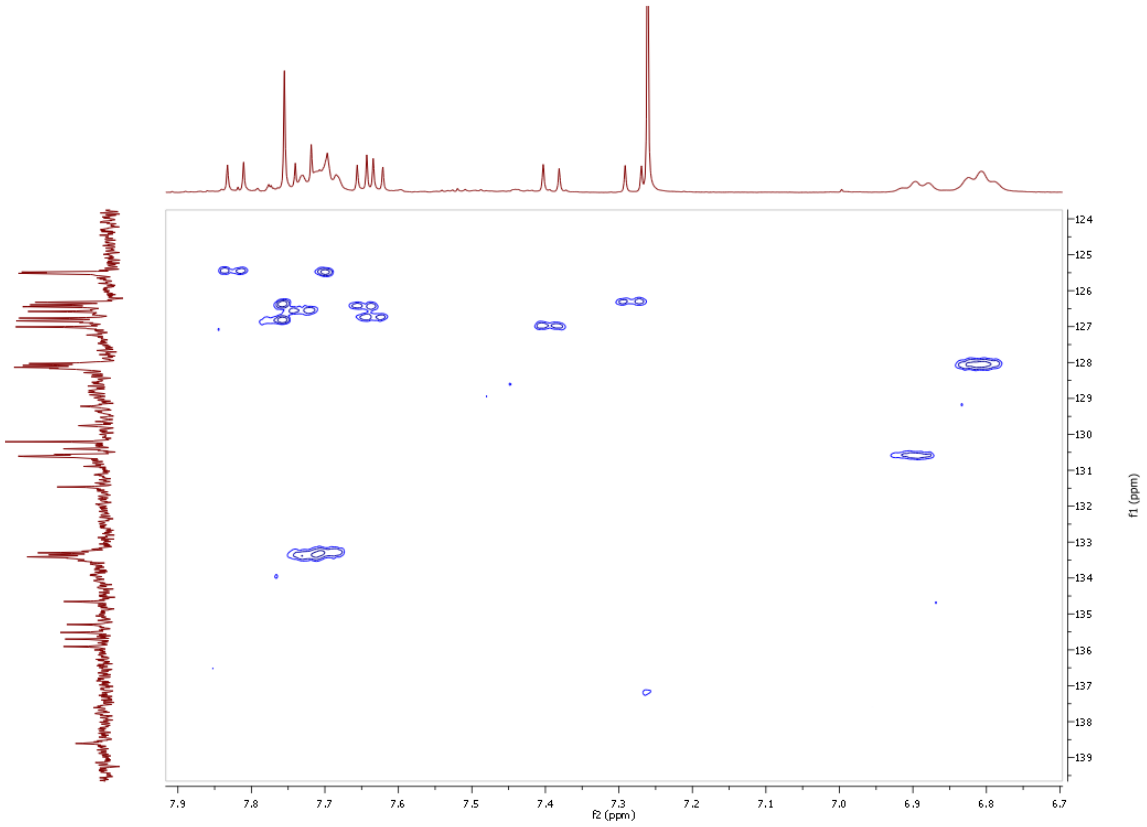

Figure S19. 2-D HSQC spectrum of Pt(dppe)(CC-CH_2-Cora)$_2$ (**4**) in $CDCl_3$.

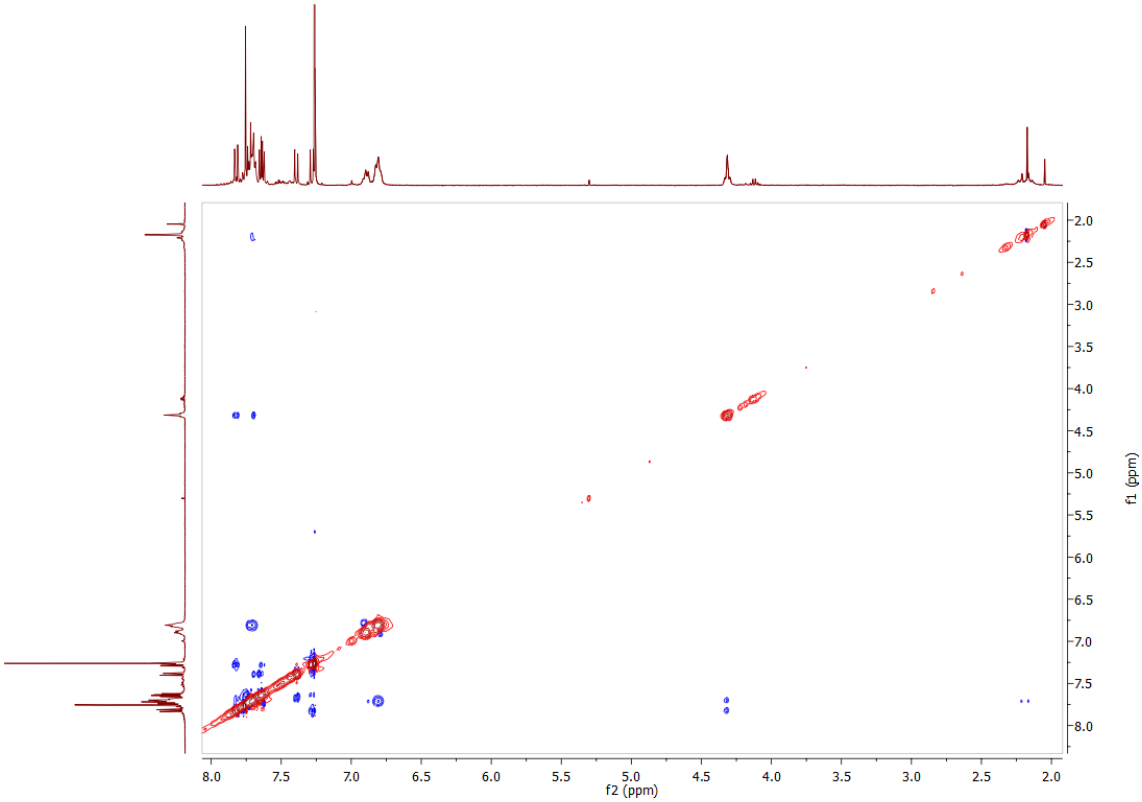

Figure S20. 2-D NOESY spectrum of Pt(dppe)(CC-CH_2-Cora)$_2$ (**4**) in $CDCl_3$.

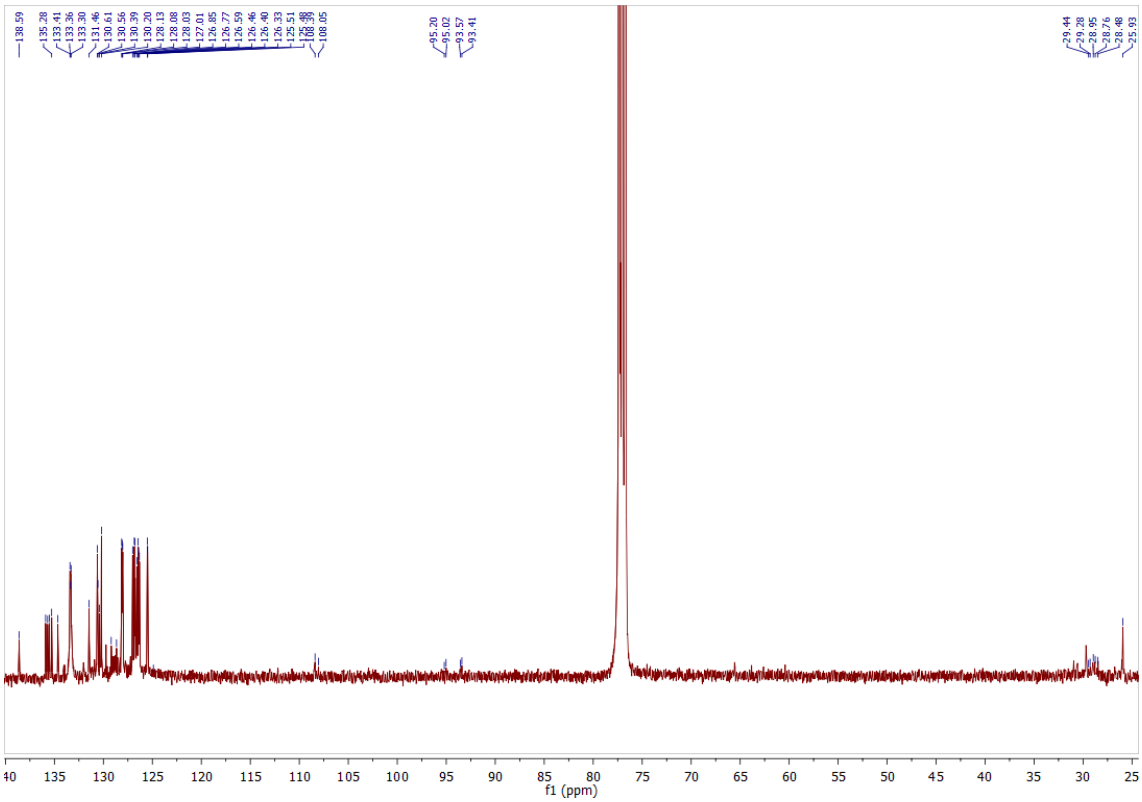

Figure S21. $^{13}C\{^1H\}$ NMR spectrum of Pt(dppe)(CC-CH_2-Cora)$_2$ (**4**) at 100 MHz in $CDCl_3$.

Job's plot experiments.

Method of continuous variation ("Job plot") was used to determine the stoichiometry of the complexation between **1** and fullerenes (C_{60} or C_{70}). Mole ratio plot of $\Delta\delta$ versus guest-to-host molar ratios confirmed the 1:1 stoichiometry in both cases (Figure S22).[5]

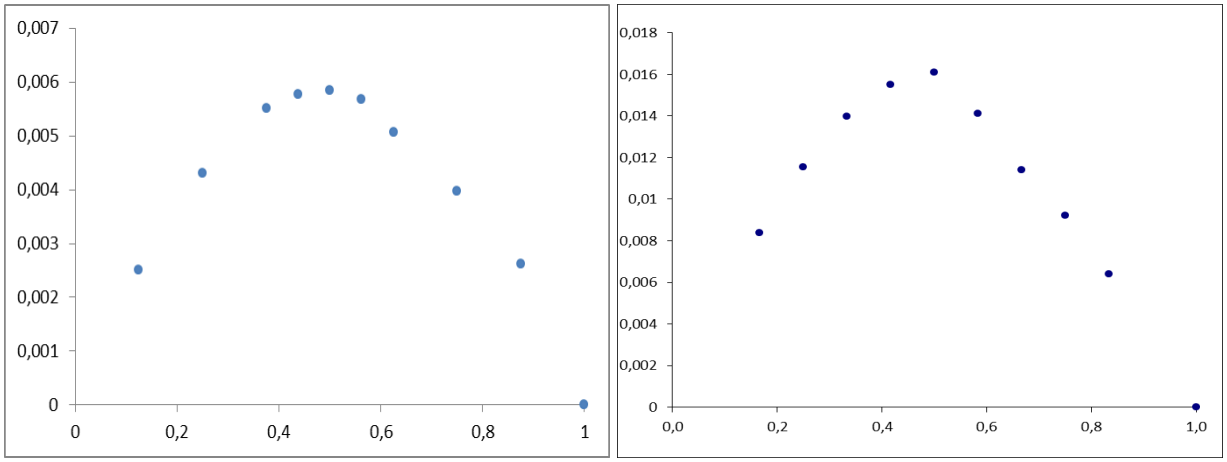

Figure S22. Job plot showing the 1:1 stoichiometry of C_{60} *vs* **1** (on the left) and C_{70} *vs* **1** (on the right).

Complexation studies of 1 with C_{60}. Titration of 1 with C60 in toluene-d_8.

The binding was investigated by ^{1}H NMR titrations. Ka was evaluated from the changes of the chemical shifts of selected independent protons of the corannulene subunits of **1**. Ka and L were optimized as parameters in the curve fitting. The Excel workbooks for curve-fitting NMR titration data of the Sanderson group (http://www.dur.ac.uk/j.m.sanderson/science/downloads.html) were employed for this purpose.

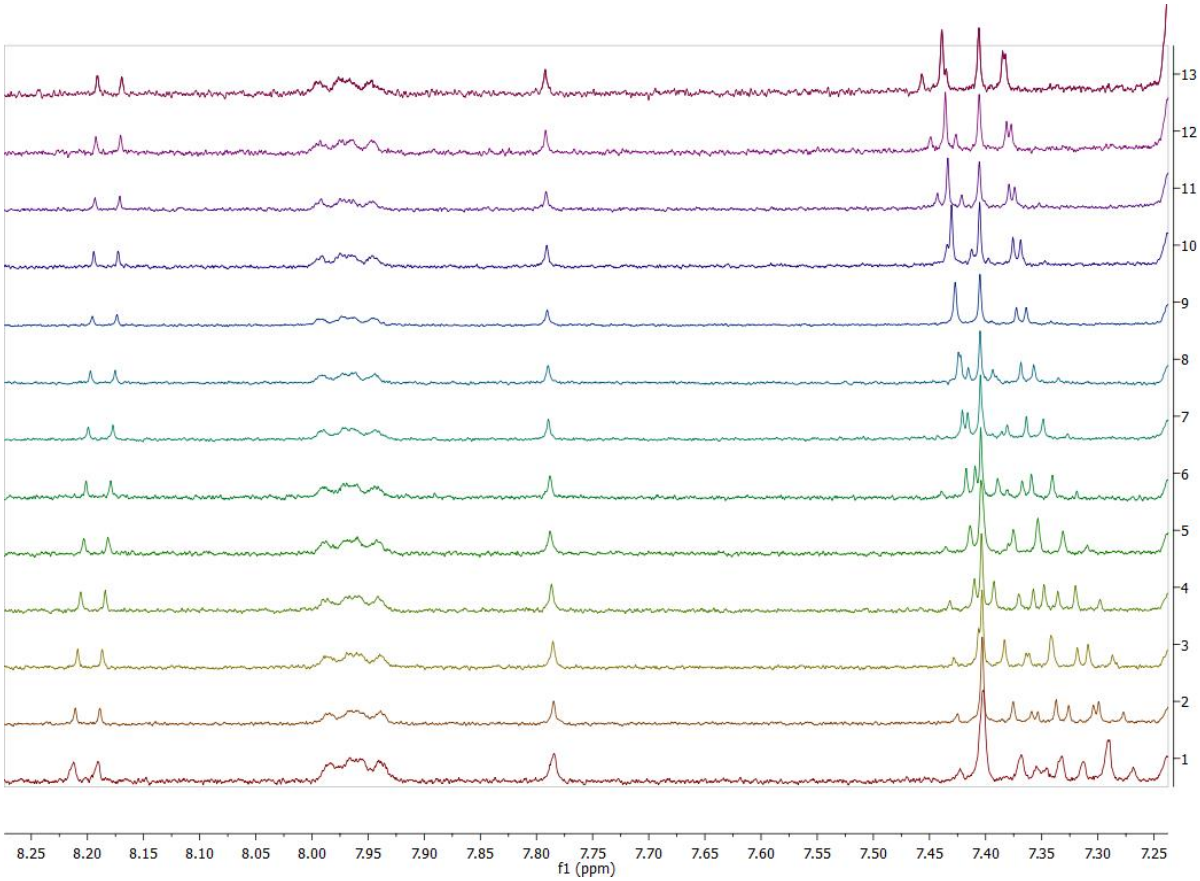

Figure S23. ^{1}H NMR titrations of [Pt(CC-Cora)$_2$(dppe)] (**1**) with C_{60} (400 MHz, 298 K, toluene-d_8).

The results of the curve-fitting for selected protons in corannulene subunits are shown below:

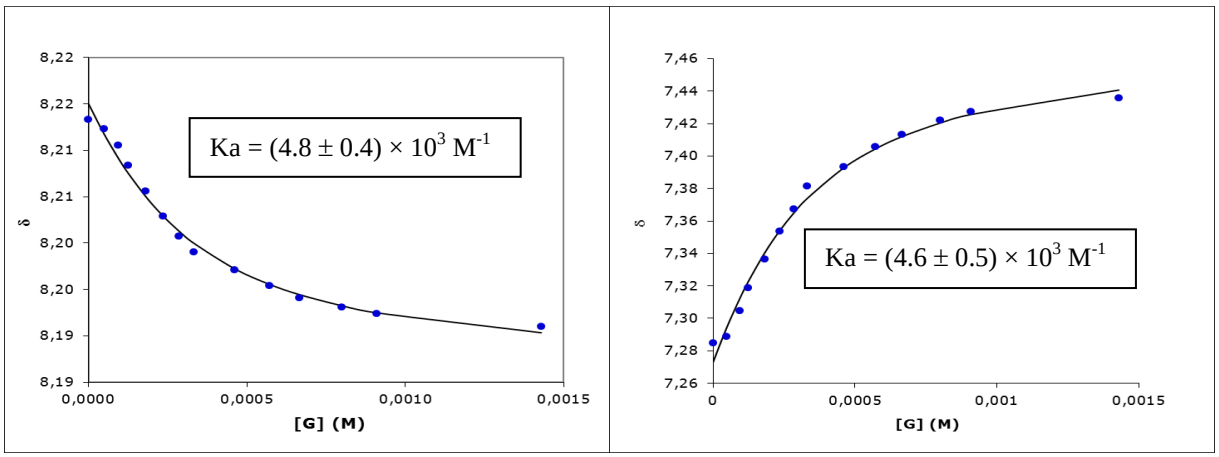

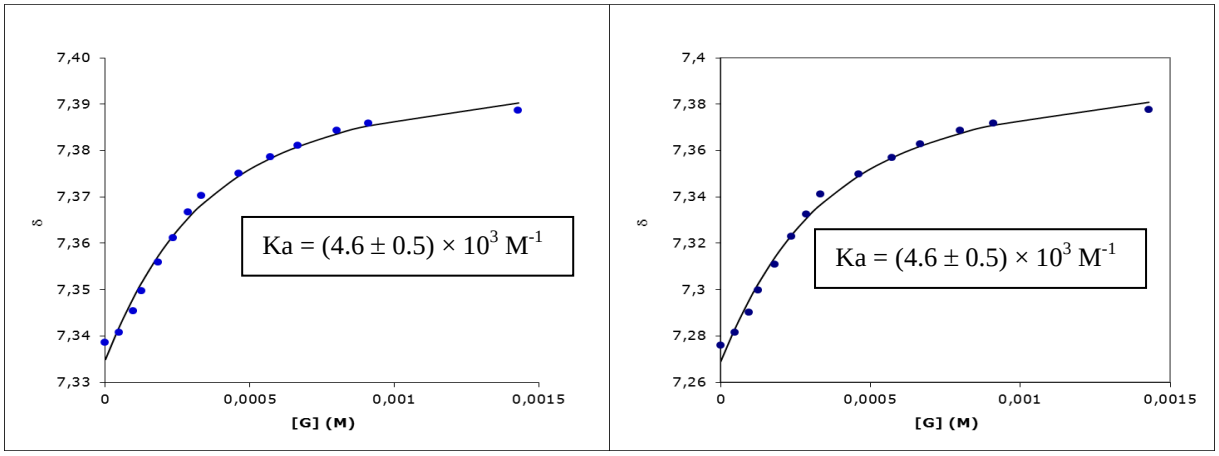

Figure S24. Non linear curve regression for the results of the titration experiments of C_{60} with **1** for selected corannulene protons (binding constant (Ka) were calculated by fitting of the chemical shifts to a 1:1 binding isotherm).

The estimated Ka values are (4.8± 0.4) × 10^3 M^{-1}, (4.6± 0.5) × 10^3 M^{-1}, (4.6± 0.5) × 10^3 M^{-1} and (4.6± 0.5) × 10^3 M^{-1} as calculated for selected corannulene protons in **1**. **The average Ka is (4.7 ± 0.5) × 10^3 M^{-1}**.

The binding was investigated by $^{13}C\{^1H\}$ NMR spectroscopy. Figure S25 shows variable temperature $^{13}C\{^1H\}$ NMR spectra for a mixture of C_{60} and **1** (1:1) in toluene-d_8. The spectra were run with sufficient number of scan to detect the signal of C_{60} only. The formation of the complex $C_{60}\subset$**1** is demonstrated by the upfield shifted of the signal of C_{60} upon cooling.

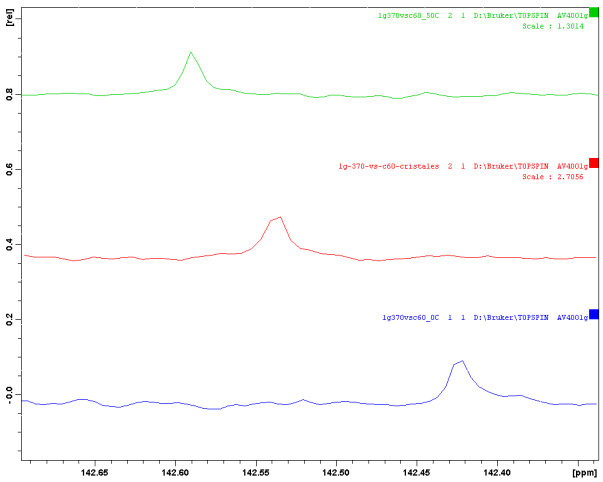

Figure S25. $^{13}C\{^1H\}$ NMR (100 MHz) spectra of a mixture of C_{60} and **1** (1:1) in toluene-d_8 at several temperatures.

The molecular ion peak of inclusion complex $C_{60}\subset$**1** can be detected using MALDI-TOF mass spectrometry as can be seen in Figure S26. The spectrum of a 1:1 mixture of **1** and C_{60}, showed peaks at *m/z* 1859.4 and 1860.4, corresponding to $[C_{60}\subset\mathbf{1}]^+$ and $[C_{60}\subset\mathbf{1}\text{-H}]^+$ (calcd.: 1859.24 and 1860.24).

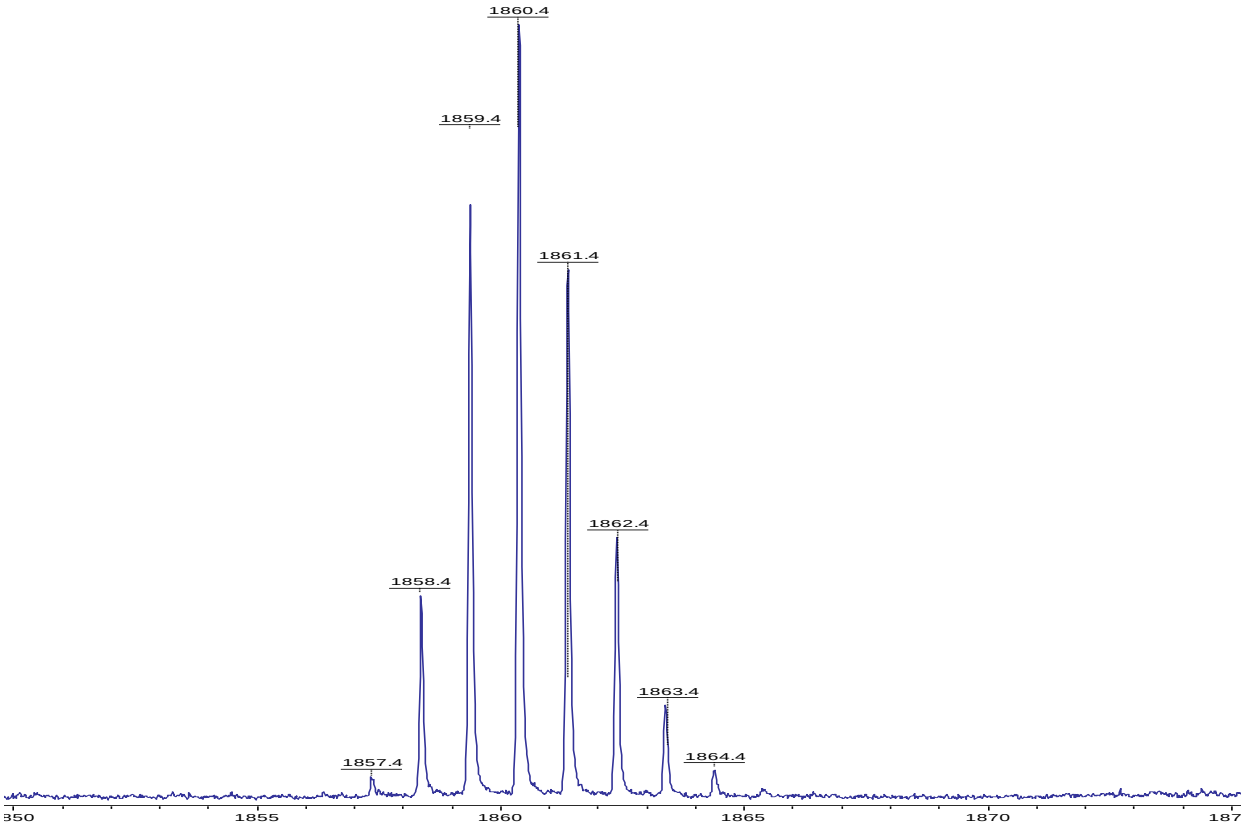

Figure S26. MALDI-TOF isotopic pattern for C60⊂**1**.

Complexation studies of 1 with C_{70}. Titration of 1 with C_{70} in toluene-d_8.

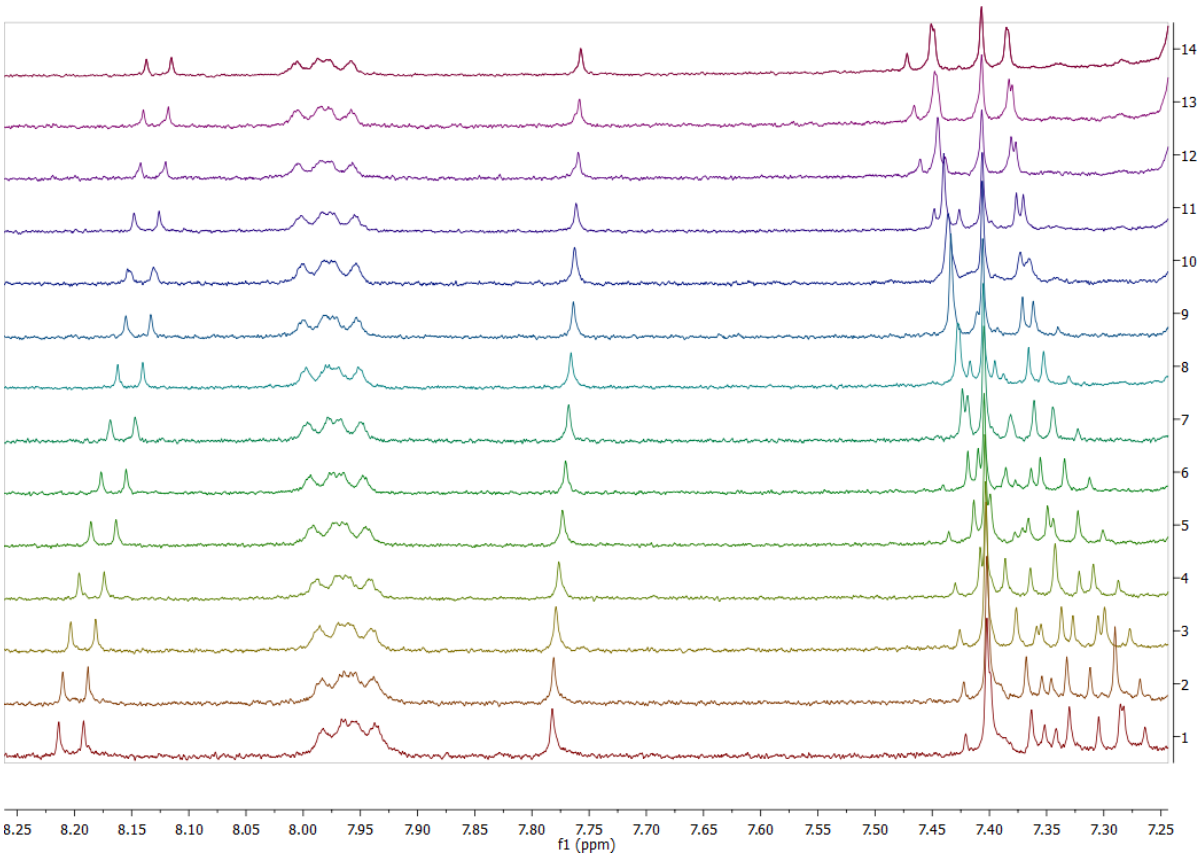

Figure S27. Partial ^{1}H NMR titrations of [Pt(CC-Cora)$_2$(dppe)] (**1**) with C_{70} (400 MHz, 298 K, toluene-d_8).

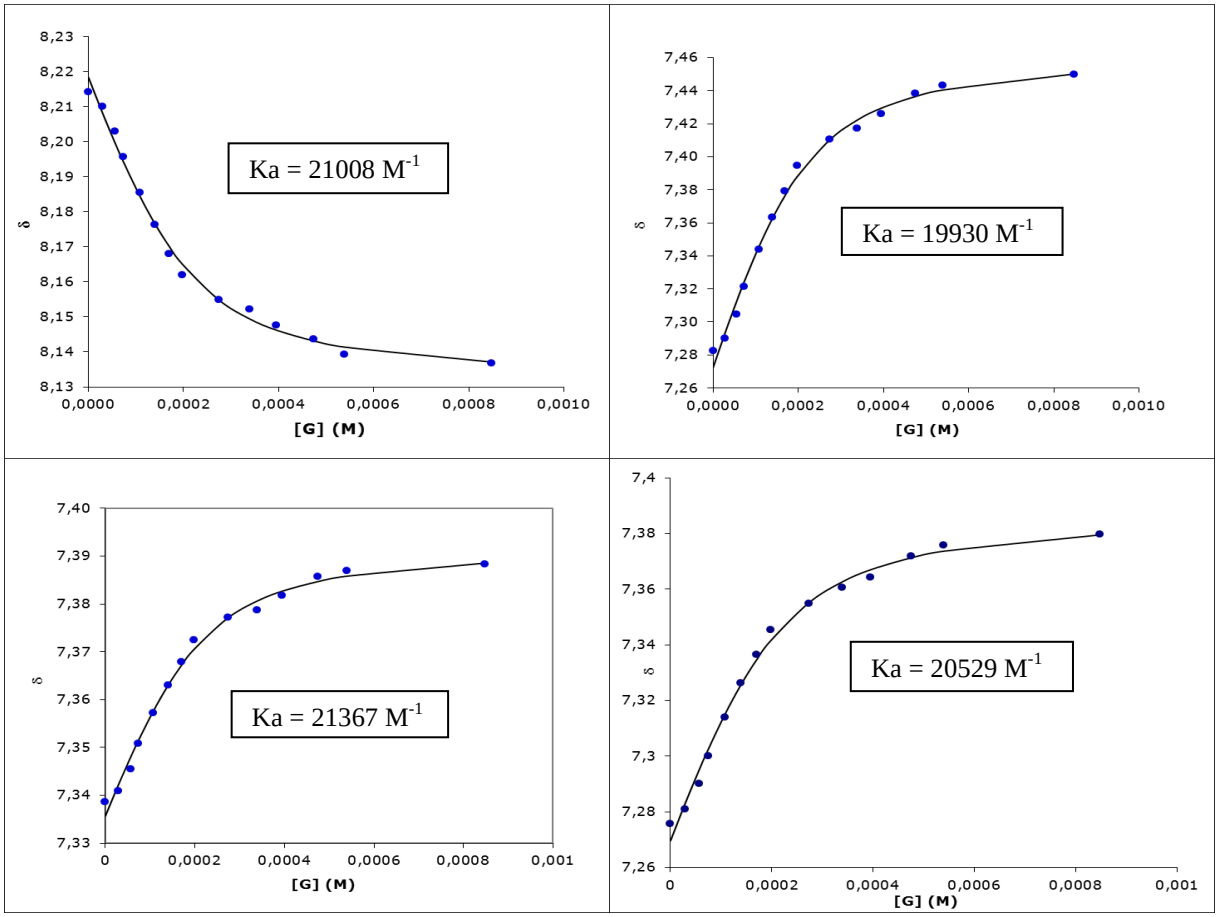

Figure S28. Non linear curve regression for the results of the titration experiments of C_{70} with **1** for selected corannulene protons (binding constant (Ka) were calculated by fitting of the chemical shifts to a 1:1 binding isotherm).

The estimated Ka values are 21008 M^{-1}, 19930 M^{-1}, 21367 M^{-1} and 20529 M^{-1} as calculated for selected corannulene protons in **1**. **The average Ka is 20708 M^{-1}**.

The molecular ion peak of inclusion complex C_{70}⊂**1** can be detected using MALDI-TOF mass spectrometry as can be seen in Figure S29. The spectrum of a 1:1 mixture of **1** and C_{60}, showed peaks at *m/z* 1979.0 and 1980.0, corresponding to $[C_{70}⊂\mathbf{1}]^+$ and $[C_{70}⊂\mathbf{1}\text{-H}]^+$ (calcd.: 1979.24 and 1980.24).

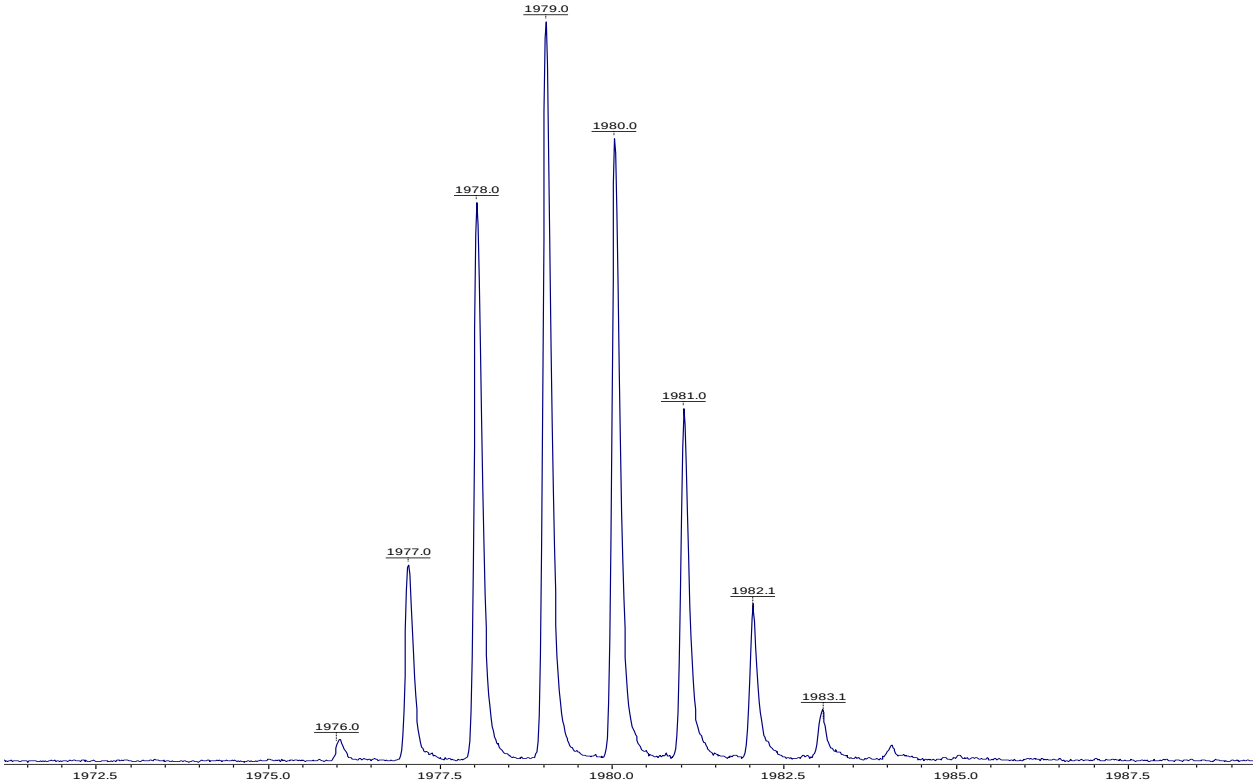

Figure S29. MALDI-TOF isotopic pattern for C70⊂**1**.

III. Crystallographic Data for C60⊂1.

Crystallographic Experimental Section.

Data collection was performed in an Agilent Supernova diffractometer with a Mo micro-focus source with multilayer optics. Data integration, scaling and empirical absorption correction was carried out using the CrysAlis Pro program package.[6] The structure was solved using direct methods and refined by Full-Matrix-Least-Squares against F^2.[7] The non-hydrogen atoms were refined anisotropically and hydrogen atoms were placed at idealised positions and refined using the riding model.

The C_{60} fragment was disordered but, for the sake of simplicity, it was modeled with just one component with the thermal parameters a little bit larger than usual. One phenyl ring, one corannulene and both toluene lattice solvent molecules were disordered. Two components were defined for each fragment and the structure converged with these final ratios for them: 55-45% for components A and B of the disordered phenyl ring, 51-49% for the two components of the disordered corannulene fragment, 65-35% for one toluene solvent molecule and 55-45% for the other toluene molecule.

SIMU restraints were applied to all C-C bonds in the disordered fragments, DELU restraints were applied to the C_{ipso}-C bonds in the two components of the disordered phenyl ring, and distances and angles of the two toluene solvent molecules were constrained with DFIX and DANG to achieve convergence of the structure.

Table S1. Crystal data and structure refinement for C60⊂**1**.

Empirical formula	C_{144} H_{58} P_2 Pt	
Formula weight	2044.93	
Temperature	293(2) K	
Wavelength	0.71073 Å	
Crystal system	Monoclinic	
Space group	C2/c	
Unit cell dimensions	a = 56.220(11) Å	α= 90°.
	b = 17.167(3) Å	β= 101.30(3)°.
	c = 19.207(4) Å	γ = 90°.
Volume	18178(6) $Å^3$	
Z	8	
Density (calculated)	1.494 Mg/m^3	
Absorption coefficient	1.642 mm^{-1}	
F(000)	8240	
Crystal size	0.45 × 0.34 × 0.10 mm^3	
Theta range for data collection	2.89 to 28.78°.	
Index ranges	$-62 \leq h \leq 73$, $-20 \leq k \leq 23$, $-26 \leq l \leq 19$	
Reflections collected	36106	
Independent reflections	19052 [R_{int} = 0.0257]	
Completeness to theta = 25.25°	99.2 %	
Refinement method	Full-matrix least-squares on F^2	
Data / restraints / parameters	19052 / 1129 / 1468	
Goodness-of-fit on F^2	0.966	
Final R indices [I > 2σ (I)]	R_1 = 0.0481, wR_2 = 0.1426	
R indices (all data)	R_1 = 0.0684, wR_2 = 0.1490	
Largest diff. peak and hole	3.156 and -0.678 e.$Å^{-3}$	

Table S2. Bond lengths [Å] and angles [º] for C60⊂**1**.

Pt(1)-C(3)	2.000(5)
Pt(1)-C(5)	2.013(5)
Pt(1)-P(2)	2.2748(13)
Pt(1)-P(1)	2.2762(14)
P(1)-C(1)	1.835(5)
P(2)-C(2)	1.839(5)
C(1)-C(2)	1.517(7)
C(3)-C(4)	1.213(7)
C(4)-C(51)	1.438(7)
C(5)-C(6)	1.181(8)
C(6)-C(119)	1.477(13)
C(6)-C(138)	1.510(14)
C(3)-Pt(1)-C(5)	90.8(2)
C(3)-Pt(1)-P(2)	89.04(15)
C(5)-Pt(1)-P(2)	177.83(15)
C(3)-Pt(1)-P(1)	174.87(15)
C(5)-Pt(1)-P(1)	94.24(13)
P(2)-Pt(1)-P(1)	85.97(4)
C(2)-C(1)-P(1)	108.9(3)
C(1)-C(2)-P(2)	109.0(3)
C(4)-C(3)-Pt(1)	171.4(5)
C(3)-C(4)-C(51)	175.1(6)
C(6)-C(5)-Pt(1)	176.3(6)
C(5)-C(6)-C(119)	161.6(9)
C(5)-C(6)-C(138)	161.7(9)

IV. Computational details.

Theoretical calculations have been carried out at the BLYP/TZP level of theory including Grimme's DFT-D3 dispersion correction,[8] as implemented in ADF 2010.[9] Relativistic effects have been included using the ZORA formalism.[10] Gradients have been smoothed and converged to 1e-2 Hartree/angstrom. The energy decomposition analysis (EDA) has been carried out at the same level of theory. Details of the method can be found elsewhere (4, 5) and only a very brief account of the main concepts will be outlined here.[11],[12] Within this procedure, the total interaction energy between two fragments is partitioned into three contributions: i) ΔE_{ES} is the classical electrostatic interaction energy between the fragments, calculated with a frozen electron distribution and using the geometry of the compound; ii) ΔE_{PAULI} arises from the exchange repulsion of the fragments' charge distributions; iii) ΔE_{ORB} is the stabilization due to orbital interactions (polarization and charge transfer). The sum of these three terms yields the ΔE_{DFT} interaction energy:

$$\Delta E_{DFT} = \Delta E_{PAULI} + \Delta E_{ES} + \Delta E_{ORB}$$

Inclusion of the dispersion contribution yields the total interaction energy, ΔE_{TOT}:

$$\Delta E_{TOT} = \Delta E_{DFT} + \Delta E_{DISP}$$

Finally, the total bond energy is obtained taking into account the preparation energy, ΔE_{DEF}, that is, the energy necessary to promote both fragments from their equilibrium geometry and electronic ground state to the geometry and electronic state they have in the molecule.

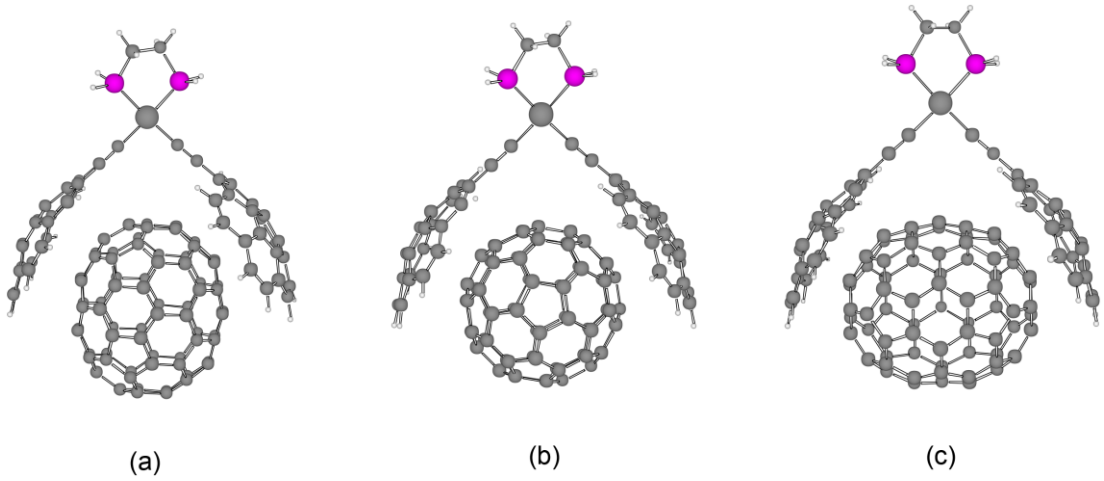

Figure S29. The three possible conformations of the **1**⊂C70 adduct as obtained at the BLYP-D3/TZP level of theory.

Table S3. Energy decomposition analysis of the adducts C60⊂**1** and C70⊂**1** performed with BLYP-D3/TZP. All contributions are given in kcal mol^{-1}.

	C_{60}⊂**1**	C_{70}⊂**1** (a)
E_{PAULI}	47,2	45,5
E_{ES}	-18,1	-17,3
E_{ORB}	-10,4	-10,3
E_{DFT}	18,6	18.0
E_{DSIP}	-53,1	-54.0
E_{TOT}	-34,4	-36,0
ΔE_{DEF}	-0.1	0.0
ΔE_{REL}	1,5	0,0

(1) (a) Mack, J.; Vogel, P.; Jones, D.; Kaval, N.; Sutton, A. *Org. Biomol. Chem.* **2007**, *5*, 2448-2452. (b) Jones, C. S.; Elliott, E.; Siegel, J. S. *Synlett*, **2004**, *1*, 187-191.

(2) Seiders, T. J.; Elliott, E. L.; Grube, G. H.; Siegel, J. S. *J. Am. Chem. Soc.* **1999**, *34*, 7804–7813.

(3) Maeda, H.; Maeda, T.; Mizuno, K.; Fujimoto, K.; Shimizu, H. Inouye, M. *Chem. Eur. J.* **2006**, *12*, 824–831.

(4) Sudhakar, A.; Katz, T. J. *Tetrahedron Lett.* **1986**, *20*, 2231-2234.

(5) Job, P. *Ann. Chim.* **1928**, *9*, 113-203.

(6) CrysAlisPro Software system, version 1.171.33.51, 2009, Oxford Diffraction Ltd, Oxford, UK.

(7) SHELX Software, Sheldrick, G. M. *Acta Cryst.* **2008**, *A64*, 112-122.

(8) Grimme, S.; Anthony, J.; Ehrlich, S. and Krieg, H. *J. Chem. Phys.* **2010**, *132*, 154104.

(9) ADF2010.02, Theoretical Chemistry, Vrije Universiteit, SCM, Amsterdam, The Netherlands; http://www.scm.com

(10) see van Lenthe, E.; Ehlers, A.E.; and Baerends, E.J. *J. Chem. Phys*. **1999**, *110*, 8943. and references therein.

(11) Bickelhaupt, F. M. ; Baerends, E. J. *Rev. Comput. Chem.* **2000**, *15*, 1.

(12) te Velde, G.; Bickelhaupt, F. M.; Baerends, E. J.; A. van Gisbergen, S. J.; Fonseca Guerra, C.; Snijders, J. G.; Ziegler, T. *J. Comput. Chem.* **2001**, *22*, 931.